

STM Investigations of Novel Porphyrinoids on Surfaces: Adsorption Behavior and Reactivity

STM Untersuchungen neuartiger Porphyrinoide auf Oberflächen:
Adsorptionsverhalten und Reaktivität

Der Naturwissenschaftlichen Fakultät
der Friedrich-Alexander-Universität Erlangen-Nürnberg
zur Erlangung des Doktorgrades Dr. rer. nat.

vorgelegt von

Michael Lepper

aus Münster

Als Dissertation genehmigt

von der Naturwissenschaftlichen Fakultät

der Friedrich-Alexander-Universität Erlangen-Nürnberg

Tag der mündlichen Prüfung: 13.04.2018

Vorsitzende/r des Promotionsorgans: Prof. Dr. Georg Kreimer

Gutachter/in: PD Dr. Hubertus Marbach

Prof. Dr. Jörg Libuda

Content

1. Introduction.....	1
2. Theoretical and Experimental Background	3
2.1 Principle and Experimental Application of STM.....	3
2.2 The Substrates	5
2.3 The Porphyrins	7
2.4 The UHV Instrument.....	11
3. Literature Review.....	12
3.1 Molecular Self-Assembly.....	12
3.2 Chemical Surface Reactions / <i>In situ</i> Metalation	16
4. Results.....	18
4.1 Intramolecular Conformation.....	19
4.2 Supramolecular Order	30
4.3 On-Surface Reactions.....	42
5. Conclusions.....	49
6. Zusammenfassung.....	51
7. Acknowledgement	54
8. References.....	55
9. Appendix.....	61
9.1 List of Figure Raw Data	61
9.2 Publications [P1-7].....	62

1. Introduction

Since the early days of science nature has been an important source of inspiration for the development of technological applications. Nowadays, due to recent technological developments in experimental and analytical techniques even fundamental biologic processes can be investigated and understood. These processes are of utmost interest because they have been optimized by evolution over millions of years yielding complex adaption of living organisms for survival in their environment. Intriguingly, one class of molecules which is deeply implemented in these vital biologic processes like photosynthesis and metabolism are porphyrins.^[1] Two prominent examples for porphyrins in nature are illustrated in Figure 1.1. In the proteins hemoglobin and myoglobin, the main functional building block enabling the oxygen transport and storage from the lung or cells of mammals is heme B, an iron(II)-porphyrin. On the other hand chlorophyll A, a magnesium(II)-porphyrin, is responsible for light harvesting and electron transfer in the photosynthesis of green plants.^[1] Obviously, the functionalities of porphyrins are strongly connected to the corresponding central metal atom. However, a contribution from the different substituents and environments must be considered as well.

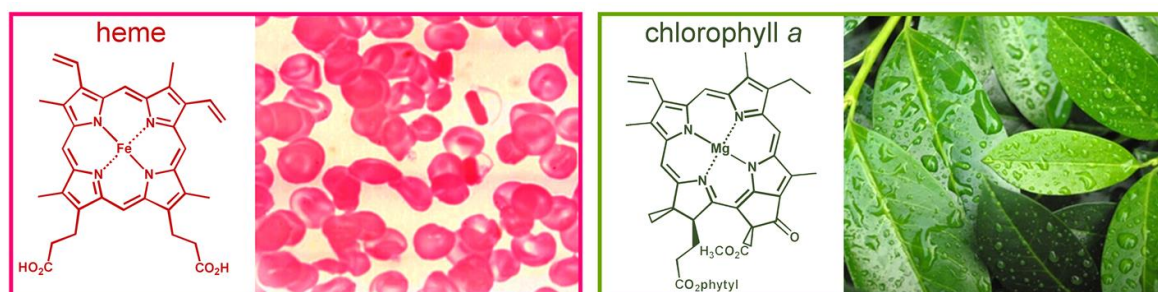


Figure 1.1 Illustration of the two most prominent metalloporphyrins in nature. Modified from ^[2].

Besides their abundance in nature porphyrins have already drawn attention for the use in technical applications like light harvesting and electron transport in solar cells,^[3-4] small molecule binding in colorimetric gas sensing^[5] and also catalysis.^[6-7] This again highlights the versatile functionality of porphyrins combining high thermal stability with flexible electronic, steric and chemical properties. The abundance of functions in nature and technology performed by porphyrins warrants the in-depth investigation of this class of molecules. In particular, since the self-assembly and adsorption behavior of porphyrins on

surfaces presents a potential pathway to the controlled fabrication of functional molecular nanostructures.^[8-10] For the investigation and characterization of these nanoscaled structures scanning tunneling microscopy (STM) has proven to be a powerful tool to gain insight into the basic chemical and physical properties. By now, porphyrins have become part of numerous surface science studies, however, a deeper understanding of the relevant fundamental processes necessary to control the formation of the molecular building blocks on the surface is still not complete.^[8-11]

The aim of the thesis at hand is to continue filling this knowledge gap by investigating and analyzing the adsorption behavior of various porphyrins on surfaces at room temperature (RT) via STM. In particular the intramolecular conformation, intermolecular interactions and supramolecular arrangements as well as on-surface reactions of tetraphenylporphyrins (TPPs) are investigated in detail.

The work at hand is a cumulative thesis based on 6 publications [P1-6] in peer-reviewed scientific journals and one publication close to submission [P7] with major contributions from the author. The work was performed in collaboration with the groups of Prof. Abner de Siervo from University of Campinas (Brazil) and Prof. Norbert Jux, Prof. Alexander Schneider, Prof. Bernd Meyer and PD Wolfgang Hieringer (all from FAU Erlangen).

First of all, the theoretical and experimental background as well as the relevant substrates and porphyrins will be briefly described. In the third chapter a short literature overview for porphyrins adsorbed on single metal surfaces is given. The main part of the thesis at hand is presented in chapter 4 and recapitulates the findings from publications [P1-7]. Finally, a conclusion is given.

2. Theoretical and Experimental Background

2.1 Principle and Experimental Application of STM

The development of the scanning tunneling microscope opened up the possibility to image conducting and semiconducting surfaces on the atomic scale in real space as well as probing local electronic states. The first suggestion for such an imaging mechanism was made by Young et al in 1972.^[12] In 1982 Gerd Binnig and Heinrich Rohrer followed up with the practical implementation of the first STM.^[13-14] The importance of their work is highlighted by the award of the Nobel prize in physics already four years later in 1986. In the meantime, STM has become an essential tool in condensed matter physics, chemistry, material science and biology. The versatility and potential of STM is also evident by the possibility to use it as a tool for fabrication of nanostructures via the manipulation of individual atoms and molecules.^[15] In the following the STM principles are reviewed. For a more detailed theoretical description the reader is referred to dedicated publications^[15-16].

The principle of STM is based on the quantum-mechanical effect of electron tunneling. It allows an electron to tunnel through a potential barrier even though in a classical physical model its kinetic energy is insufficient to overcome the barrier. In quantum-mechanics the electron can be described by its wave function Ψ . Even within the potential barrier Ψ is not 0 but exhibits an exponential decay. Therefore, $|\Psi^2|$, which is the probability density to find the electron at a certain position, is also not 0 enabling “tunneling” through the potential barrier. In the case of STM the potential barrier is given by the gap between tip and sample. Based on this effect, STM is capable of probing the topography and the electronic structure of a flat sample surface with a sharp conducting, ideally monoatomic tip. Commonly, the tip is made from tungsten or 90:10 platinum:iridium alloy and is mounted on a piezoelectric scanning unit allowing precise control in x , y and z direction. For these specific movements the piezo actuators are used based on the reverse piezoelectric effect, i.e., they translate electric signals into mechanical motion typically down to the sub Å range up to a few μm .^[17]

For measurement the tip is approached towards the surface until a certain tunneling current I is established. Typically, the distance d between tip and sample is in the sub-nm regime for tunneling “contact”. The dependency of the tunneling current I can be described by the simplified proportional correlation:^[18]

$$I \propto V \cdot e \frac{-2d}{\hbar} \sqrt{2m_e \Phi} \quad (2.1)$$

In this equation Φ represents the barrier height between tip and sample, which is, in a first approximation, the averaged value of the work functions of tip and sample. Furthermore, m_e is the mass of an electron and V is the applied bias voltage between tip and sample. The exponential decay of the tunneling current I with increasing distance d emphasizes the extreme height sensitivity of STM which allows to gain information on the sample topography in the sub-Å regime. It should be kept in mind that the local density of states (LDOS) of the sample are probed in STM. The LDOS usually reflects the topography of the investigated structure but in specific cases the electronic structure has a significant influence on the STM image such that it deviates from the expected topography. This is often reflected in a bias dependent appearance in STM.^[19-20] These fundamental relations are then utilized by raster-scanning the surface in order to obtain an image of the sample surface. Generally, two main measurement modes can be distinguished, namely: constant-current and constant-height mode. In the latter the vertical tip position (z) is kept constant while the tunneling current I is recorded vs the lateral tip position to obtain the corrugation of the surface. The upside of this operation mode is high scanning speeds, since no response from a feedback loop is required. However, it is limited to very flat surfaces because a large surface corrugation can cause crashes of the tip. In the more commonly used constant-current mode the vertical tip position is adjusted by a feedback controller in a way that the tunneling current is kept constant. Thus, an image of the surface can be reconstructed by the vertical tip position (z) vs. the lateral position (x, y). Even though this mode is more time consuming than the constant-height mode it allows for the measurement of comparatively rough surfaces.

For all STM measurements in the thesis at hand the given bias voltages refer to the sample and the images are recorded in constant-current mode. WSxM^[21] is used for processing of the STM raw data, with moderate low pass filtering and background subtraction being typically applied for noise reduction.

2.2 The Substrates

In the thesis at hand the adsorption behavior of various porphyrins adsorbed on copper and silver single crystal surfaces is investigated by STM. These studies demand detailed knowledge of the atomic arrangement and the electronic and chemical structure of the substrate. As illustrated in Figure 2.1, both copper and silver crystallize in the face centered cubic (fcc) lattice, typical for many coinage metals. The bulk lattice parameter is 0.361 nm for Cu and 0.408 nm for Ag. For the close-packed $\langle 111 \rangle$ plane indicated green in Figure 2.1 a) the next neighbor distance is 0.255 nm and 0.289 nm for Cu and Ag, respectively (see also Figure 2.1 b)).

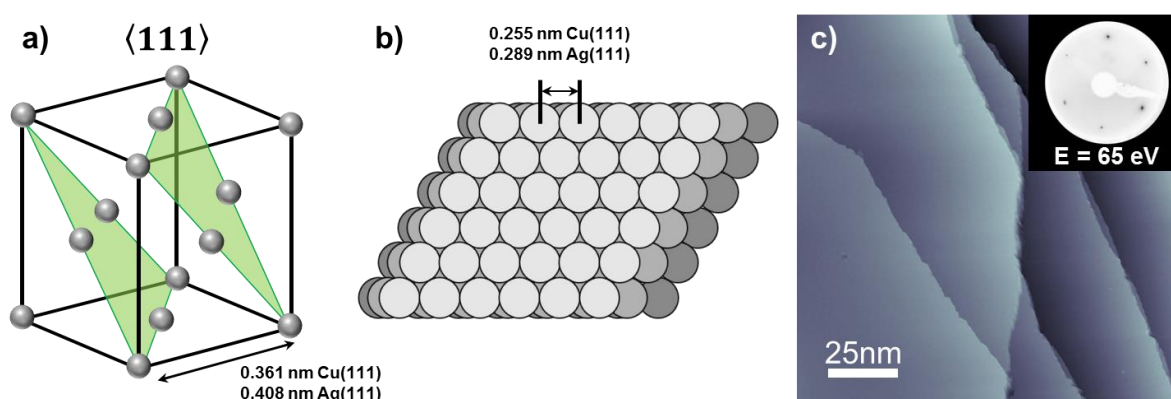


Figure 2.1 (a) Face centered cubic (fcc) unit cell with indicated $\langle 111 \rangle$ plane in green. (b) topview of the $\langle 111 \rangle$ plane. (c) STM image of a clean Cu(111) surface and the corresponding LEED image shown in the insert. Tunneling parameters: (c) $U_{\text{bias}} = -1 \text{ V}$, $I_{\text{set}} = 29 \text{ pA}$

Figure 2.1 c) depicts a STM image of a clean Cu(111) surface showing large flat terraces and step edges. The corresponding low energy electron diffraction (LEED) pattern, depicted in the insert in Fig 2.1 c), exhibits six sharp diffraction spots in a hexagonal arrangement evidencing the long range three-fold symmetry of the $\langle 111 \rangle$ surface. The Cu(111) single crystal was purchased from *MaTeck* while the Ag(111) crystal was purchased from *Surface Preparation Laboratory*. While both Ag(111) and Cu(111) exhibit the same surface geometry, the Cu substrate is considered as the chemically more reactive substrate. By comparing experiments on both surfaces the role of the substrate for the adsorption behavior of porphyrins can be evaluated.

2. Theoretical and Experimental Background

In addition, experiments were conducted on Cu(110) and the Cu(110)-(2x1)O reconstructed surface. Figure 2.2 a) and b) depict the $\langle 110 \rangle$ plane and the corresponding top view giving again a next neighbor distance of 0.255 nm and a row distance of 0.361 nm. The top view of the oxygen reconstructed Cu(110)-(2x1)O surface is shown in Figure 2.2 c). The Cu(110) crystal was purchased from Mateck. In comparison to the (111) surfaces, the Cu(110) surface is considered even more reactive substrate due to its “open” structure enabling stronger adsorbate – substrate interactions.^[22-23] On the other hand, the (2x1)O reconstructed surface exhibits a modified reactivity relative to a bare Cu(110) surface due to the different structure and presence of oxygen atoms.^[24]

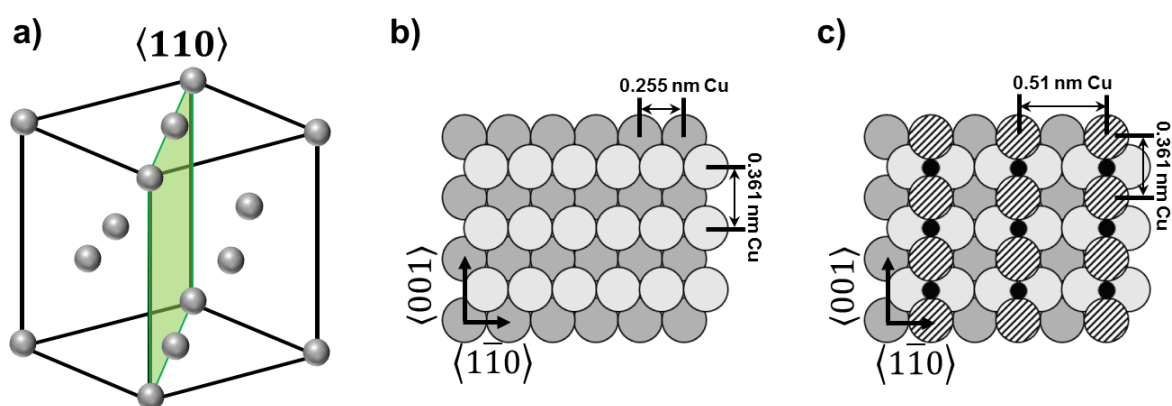


Figure 2.2 (a) Face centered cubic (fcc) unit cell with indicated $\langle 110 \rangle$ plane in green. (b) topview of the $\langle 110 \rangle$ plane. (c) topview of the Cu(110)-(2x1)O reconstructed plane. Oxygen atoms are black.

The crystals have a specified purity of >99.99 % and an alignment of $<0.1^\circ$ with respect to the nominal orientation. Basic preparation of the crystals is realized by repeated cycles of Ar^+ -ion sputtering (500 eV, sample current between 2-3 μA) at an Ar background pressure of 5×10^{-5} mbar and annealing to 850 K. The annealing step is programmed to follow a temperature rate of 1 K/s to 850 K and then keeping this temperature for 10 minutes followed by cooling down to RT with a rate of 0.3 K/s. By this rather slow preparation procedure the size of terraces can be increased while the number of step edges is reduced. For Cu(111) and (110) the manipulator was cooled down and kept at around 170 K during the annealing procedure to prevent contamination of the sample surface by desorbing species from the manipulator (for more details refer to ^[25]).

Preparation of the Cu(110)-(2x1)O reconstructed surface was achieved by dosing O₂ (600 Langmuir, 1 L = 1.3 x 10⁻⁶ mbar s, purity = 99.99%), whilst keeping the sample temperature at 500 K.

2.3 The Porphyrins

The chemical structure of porphyrins displays a central, reoccurring feature (marked red in Fig 2.3). This macrocycle consists of four pyrrole rings linked by four methine bridges.^[1] As indicated by the schematic drawing in Figure 2.3, porphyrins exhibit extended, highly conjugated π -systems with the macrocycle obeying Hückel's rule for aromaticity.^[26] The porphyrin center can host two hydrogen atoms referred to as free-base or 2H-porphyrins (Figure 2.3 a)). This configuration yields two iminic (without hydrogen) and two aminic (with hydrogen) nitrogen atoms in the pyrrole rings. Equal coordination of a metal center to all four nitrogen atoms leads to the formation of metal-porphyrins (Figure 2.3 b)).

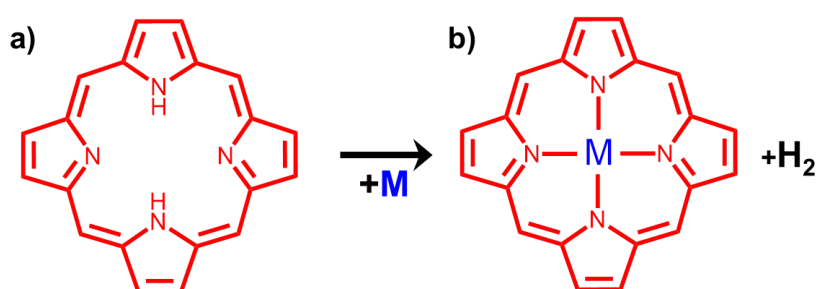


Figure 2.3 Schematic drawing of free-base porphyrin (a) and the corresponding metalated species (b).

A wealth of possible substituents can be attached to the macrocycle in various positions leading to numerous possible porphyrin derivatives. The porphyrins investigated in the thesis at hand are depicted in Figure 2.4.

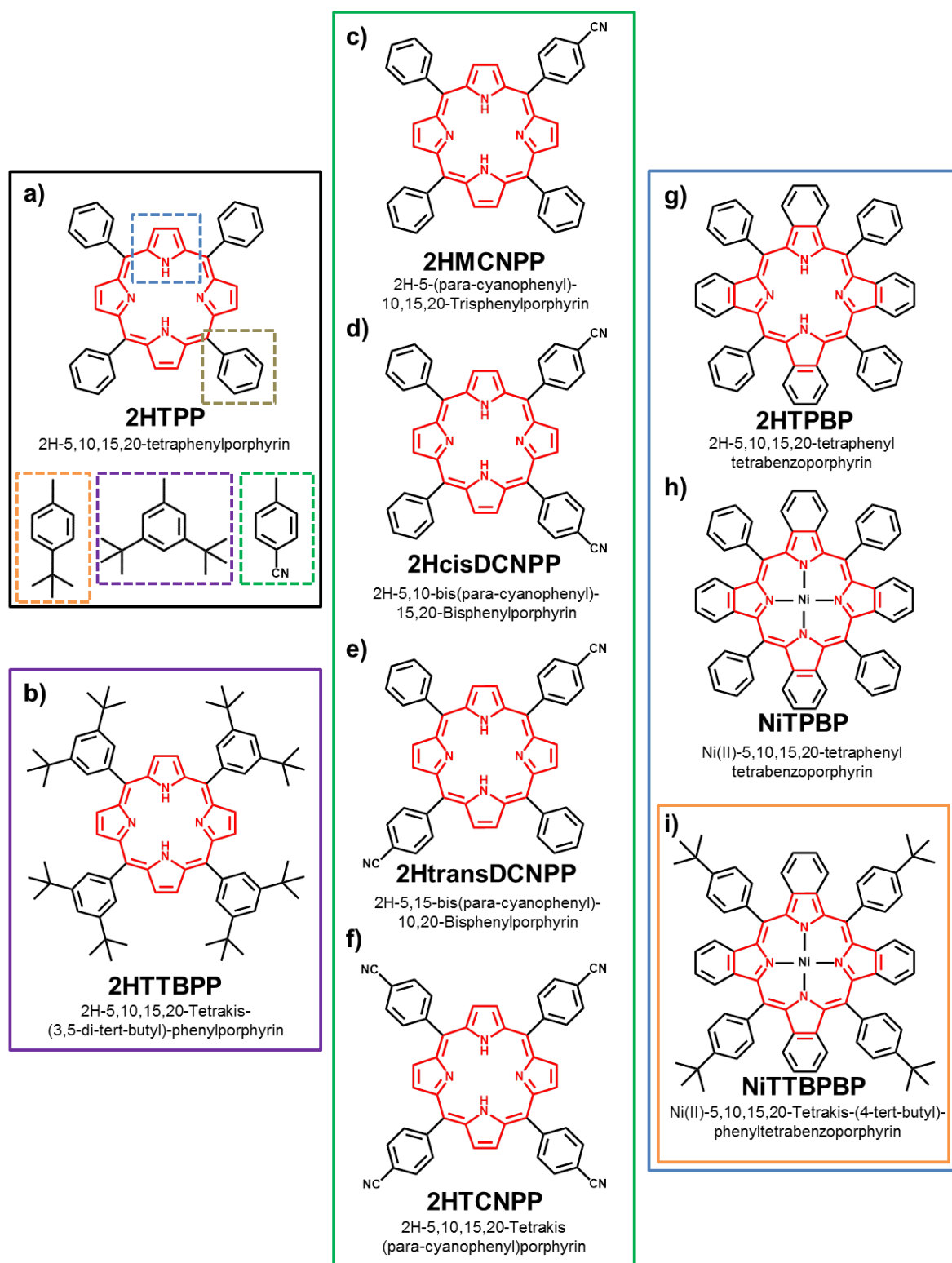


Figure 2.4 Schematic drawing of the porphyrins investigated in the thesis at hand. The recurring building block is marked red.

Porphyrin nomenclature is complex and inconsistent in literature. The following, most common nomenclature will be used to describe the porphyrins investigated in the thesis at hand. Two main types of substitution sites, as marked in Fig 2.4 a), can be distinguished: substituents bound to the methine bridges which interconnect the pyrrole groups of the macrocycle are referred to as *meso*-substituents (brown). As a second possibility the pyrrole groups themselves can be substituted at the β -positions (blue).^[27]

All of the molecules in Figure 2.4 are substituted with phenyl legs at all four *meso*-positions, marked brown in Fig 2.4 a). Therefore, these molecules are trivially referred to as “tetraphenylporphyrins”. As depicted in the lower part of Fig 2.4 a), the groups used to additionally functionalize the porphyrins in *meso*-position constitute (4-*tert*-butyl)-phenyl (orange), (3, 5-di-*tert*-butyl)-phenyl (purple) and *para*-cyanophenyl groups (green).

Due to the functionalization with cyano groups at the *para*-positions of the *meso*-substituted phenyl legs the molecules shown in the middle panel of Figure 2.4 (c-f) are termed “cyanoporphyrins”.

Fourfold functionalization directly at the β -positions of the macrocycle, marked blue in Fig 2.4 a), with benzene rings gives the name “tetrabenzoporphyrins”. The tetrabenzoporphyrins relevant for the thesis at hand are shown in the rightmost panel of Figure 2.4 (g-i).

From the schematic drawings one might anticipate that the tetraphenylporphyrins exhibit a rather flat intramolecular conformation. However, the orientation of the individual groups within the molecules deviates from this flat geometry, especially if adsorbed on a surface. The molecular conformation of porphyrins is a main part of the thesis at hand and will be discussed in more detail later on. However, some general information on the possible geometrical flexibility and the associated angles will be introduced at this point. Figure 2.5 illustrates that the internal conformation can be described by the following: the twist angle θ representing the rotation of the phenyl legs around the σ -bond, the tilt angle ϕ corresponding to the inclination of the phenyl legs out of the macrocycle plane and the angle δ describing the tilting of the pyrrole groups out of the macrocycle plane.^[28-32]

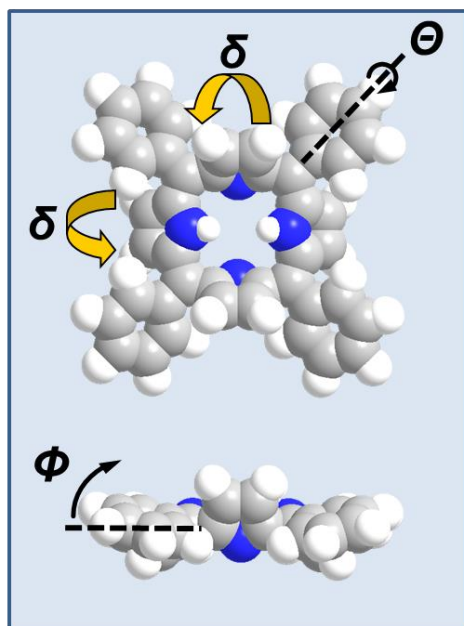


Figure 2.5 space filling model of 2HTPP illustrating the conformational flexibility of porphyrins. The angles θ and ϕ correspond to the twist and tilt angle of the phenyl legs. The angle δ refers to the tilting of pyrrole groups out of the macrocycle plane.

In the intramolecular conformation illustrated in Figure 2.5 two opposite pyrrole groups are tilted upwards and the other two downwards while the phenyl legs are twisted as well. This so-called “saddle shape” conformation has been proposed for several porphyrin molecules adsorbed on metal surfaces and has been attributed to attractive molecule-substrate interactions and steric repulsion of phenyl legs and pyrrole groups.^[33-39] The conventional saddle shape conformation as well as a novel adsorption geometry found in the course of the thesis at hand will be discussed in more detail in chapter 3 and 4.

The 2HTPP material was purchased from *Porphyrin Systems* with a specified purity of 98%. The other porphyrin compounds (see Figure 2.2) were synthesized by the group of Prof. Norbert Jux from the Chair of Organic Chemistry II at the Friedrich-Alexander-Universität Erlangen-Nürnberg. The investigated porphyrin layers were deposited on the single crystal surfaces held at RT by thermal sublimation from a home build Knudsen cell.^[40]

2.4 The UHV Instrument

All experiments and the sample preparation were performed in a two chamber UHV-system with a base pressure in the low 10^{-10} mbar regime. One chamber houses the scanning tunneling microscope (STM chamber) while the other chamber is dedicated to sample preparation. The whole set-up rests on three *Newport I-2000* laminar flow stabilizers to isolate against external low frequency vibrations. In the following the components of the UHV instrument will be described briefly; for further description and details the reader is referred to earlier reports^[41-42].

The preparation chamber provides various sample preparation and characterization components: a *SPECS IQE11/12* sputter gun and electron bombardment heating to clean and anneal the substrates. Two Knudsen cell evaporators are used for deposition of organic materials. Both evaporators can be individually pumped and separated from the chamber by gate valves allowing fast exchange of deposition material without breaking the vacuum of the preparation chamber. For metal deposition an *Omicron Focus EFM 3* electron beam evaporator is attached to the chamber. Additionally, several gas inlets offer the possibility of dosing gas into the chamber. For sample characterization, *SPECS ErLEED* optics for low energy electron diffraction (LEED) and a *Pfeiffer HiQuad QMG700* ($m/z = \text{max. } 2000$) mass spectrometer to detect large organic molecules (such as porphyrins) are installed.

The STM chamber houses a commercial *RHK UHV VT STM 300* scanning tunneling microscope following the Besocke STM design.^[43] The sample temperature can be controlled via radiative heating and a flow cryostat in a temperature range from ~ 200 up to 500 K. The STM is controlled by *SPM 1000* electronics from RHK Technologies. A variable gain low noise current pre-amplifier (*FEMTO DLPCA-200*) is equipped to measure low tunneling currents in the range of 10 – 50 pA.

3. Literature Review

3.1 Molecular Self-Assembly

As described in what is now known as Moore's law, the miniaturization trend in the semiconductor industry is such that the number of transistors per area on integrated circuits is doubled every two years.^[44] However, this trend faces imminent size restrictions in atomic dimensions which cannot be overcome by the common lithographic techniques applied in industry. Therefore, a major focus of surface science lies on the controlled fabrication of functional nanostructures. Therein the two main routes, namely top-down and bottom-up approach, can be distinguished. In the top-down approach larger components are used to fabricate structures from smaller entities. This miniaturization technique is realized, e.g., via classic lithographic methods and is up to now state-of-the-art in semiconductor industry. On the other hand the bottom-up approach enables the assembly of complex structure from small building blocks (atoms and/or molecules) in a controlled manner.^[9] It therefore presents a possibility to overcome the limitations of the top-down approach and to satisfy the increasing demand for miniaturization. The bottom-up approach is inspired by and utilizes a concept found in nature, namely the realization of an arrangement by molecular recognition in a self-assembly process. Whitesides et al. define molecular self-assembly as "spontaneous association of molecules under equilibrium conditions into stable, structurally well-defined supramolecular architectures joined by non-covalent bonds on surfaces".^[45] This process has the potential to tailor highly organized nanoarchitectures through the formation of supramolecular structures with long-range order. However, this demands detailed knowledge of the fundamental processes, in particular, adsorbate-adsorbate and adsorbate-substrate interactions. In that regard porphyrins certainly belong to the most promising candidates not only as model system but as functional molecular building blocks.^[8, 10, 46] Furthermore porphyrins offer a broad range of derivatives with tunable properties due to the availability of a wide variety of substituents.^[34, 46]

In general porphyrins tend to adsorb flat lying on the substrate driven by van der Waals forces, i.e. with the plane of the macrocycle oriented parallel to the surface.^[46-47] However, in many cases coplanar alignment of the peripheral substituents with the flat macrocycle is sterically hindered. One exemplary group for this behavior are tetraphenylporphyrins (TPPs) which present a heavily investigated and well-known model system featuring four phenyl

rings in the periphery attached to the porphyrin macrocycle (c.f. Fig 2.4a)).^[8, 10, 34, 46] For TPPs the rotation of the peripheral phenyl legs in the plane of the macrocycle is sterically hindered which is proposed to lead to a somewhat distorted, so-called saddle shape conformation (c.f. Fig. 2.5).^[33-36] Intriguingly, by changing the molecular structure the intramolecular conformation can be influenced as well. For example by introducing rather bulky *tert*-butyl groups to the phenyl legs of TPPs a “bowl” like structure was observed for 2H-Tetrakis-(3,5-di-*tert*-butyl)-phenylporphyrin (2HTTBPP) on Cu(111).^[31] However, the molecular structure is not only determined by the substituents but also by the macrocycle and the corresponding interaction with the surface. As mentioned before, van der Waals interactions have been identified as the dominating molecule-substrate interactions while more specific chemical bonds have often been disregarded.^[36] In a recent study Albrecht et al. found a peculiar conformation of 2H-tetraphenylporphyrin (2HTPP) on Cu(111) which shows a strong distortion of the macrocycle with two pyrrole groups almost perpendicular to the surface.^[48] This conformation indicates strong interaction of the free-base porphyrin macrocycle with the surface and makes a clear case for localized, specific chemical bonds. Publication [P5] addresses this issue and enables further insight in to this peculiar interaction. In conclusion, the intramolecular conformation of porphyrins is strongly correlated to their molecular structure and the corresponding interaction to the substrate. However, the intramolecular interaction is also linked to molecule-molecule interactions.^[10]

In a bigger picture, the changes induced by functionalization of porphyrins are not only limited to their intramolecular conformation but are also apparent on the supramolecular scale. Already small modifications of the peripheral substituents potentially open up different intermolecular interactions which can result in substantially different supramolecular order.^[8, 10, 34, 46] This can be exemplarily demonstrated by comparing 2HTPP and 2H-tetraphyridylporphyrin (2HTPyP) on Ag(111) which exhibit only a subtle difference in their chemical structure, i.e., in the periphery of the molecule the *para*-positioned carbon atom of each phenyl substituent is replaced by a nitrogen atom. Interestingly, 2HTPP molecules arrange in a long-range square order^[41] whereas for 2HTPyP molecules a herringbone structure is observed.^[49] Naturally this correlation of molecular structure and supramolecular order bears the potential for tailoring molecular nanostructures. However, to do so, the strong influence of the substrate on the adsorption behavior has to be considered as well: As already mentioned, 2HTPP molecules on Ag(111) form self-assembled structures consisting of well-ordered, square unit cells governed by intermolecular interactions.^[35] On the other hand,

2HTPP molecules on the presumably more reactive Cu(111) substrate adsorb individually and are exclusively oriented along the crystallographic main directions of the substrate but without supramolecular order at low coverages at RT.^[38, 50] This significantly different adsorption behavior of the same molecule on different substrates is based on a complex interplay of molecule-molecule and molecule-substrate interactions as illustrated in Fig 3.1. The depicted molecule models exhibit the state-of-the-art saddle shape adsorption geometry.

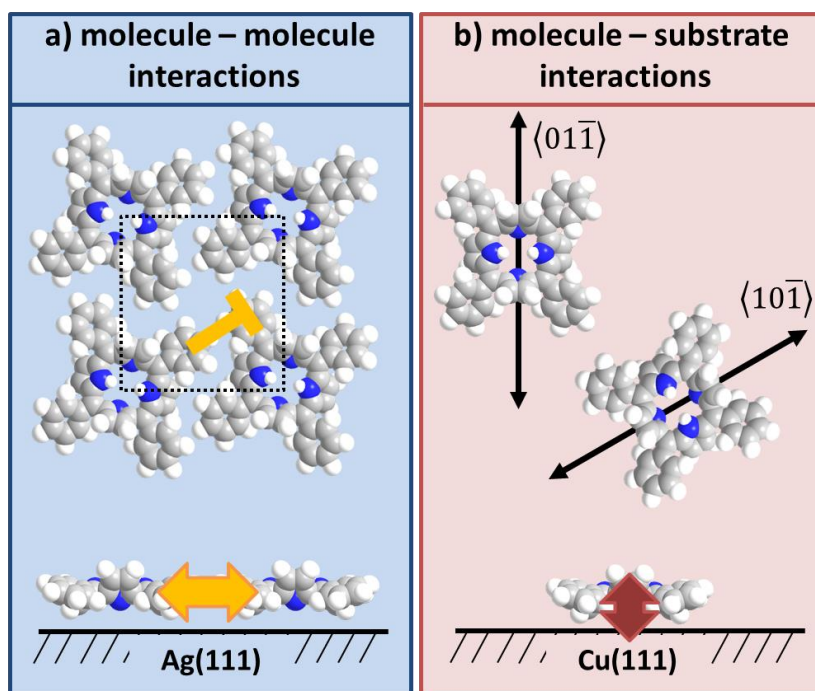


Figure 3.1 Illustration of the adsorption behavior of 2HTPP on (a) Ag(111) and (b) Cu(111). On Ag(111) the adsorption behavior is dominated by intermolecular interactions (T-type) leading to 2D supramolecular arrangements. On Cu(111) individual, isolated molecules oriented with the crystallographic main directions of the substrate are observed due to a strong molecule-substrate interaction.

On weakly interacting substrates like Ag(111) or Au(111) free-base porphyrins exhibit high mobility at RT.^[10, 35, 49-50] Mutual stabilization of the molecules on the surface is accomplished by dominating intermolecular interactions leading to the formation of two-dimensional supramolecular arrangements. In that regard, a certain type of interactions characteristic for aromatic groups, namely “T-type” interactions of the peripheral phenyl legs, as indicated with orange in Fig 3.1, have been referred to as the stabilizing interactions.^[35, 51] For 2HTPP on Cu(111) the system is dominated by molecule-substrate interactions which is

reflected by low mobility of the molecules and hindrance to form well-ordered structures. The fixation of the molecules to the crystallographic main directions prohibits the formation of stabilizing T-type interactions. Another reason for the absence of stabilizing intermolecular interactions is a deviation of the adsorption geometry from the up-to-now assumed saddle shape due to strong molecule-substrate interactions. The nature of the strong coordinative bond of free-base porphyrins to the Cu substrate has been discussed in previous studies and is part of [P5] and therefore will be discussed in more detail in chapter 4.1.^[38, 48, 52]

So far, supramolecular order of porphyrins induced by non-covalent intermolecular interactions has been discussed. However, supramolecular order of porphyrins on surfaces can also be achieved by covalent linking. Grill et al. have demonstrated that bromine-functionalized porphyrins can be covalently connected *in situ* by thermal activation in an on-surface Ullmann reaction.^[53] Obviously, this type of coupling does not fit the classic definition of self-assembly by Whitesides but nevertheless presents a suitable way to generate supramolecular arrangements. Further *in situ* generation of supramolecular arrangements has been demonstrated by Haq et al. who demonstrated porphyrin linkage by C-Cu bond formation after thermal activation without the need of additional functionalities.^[54-55]

A novel way to influence the supramolecular order *in situ* was utilized in the thesis at hand. As described in chapter 4.2, it is possible to form metal-organic coordination frameworks of porphyrins by introducing CN groups to the periphery of tetraphenylporphyrins. In general, cyano groups are of great interest for self-assembly since they promote different binding motifs, namely: H-bonding, dipolar coupling and metal organic bond formation.^[56-59]

In conclusion it can be stated that molecular self-assembly of large organic molecules on well-defined surfaces bears great potential for the design and tailoring of functional nanostructures. However, in order to achieve this goal detailed knowledge concerning the complex interplay of molecule-molecule as well as molecule-substrate interactions is indispensable.

3.2 Chemical Surface Reactions / *In situ* Metalation

The *in situ* metalation of free-base porphyrins with metal atoms from the substrate or with pre- and postdeposited material has received increasing attention in surface science due to the versatile functionality of the metal center in porphyrins.^[8, 10-11, 60] The latter can not only influence the electronic structure of the macrocycle but also act as an active site, e.g., for the adsorption of small molecules^[61] and catalytic reactions.^[62] By now the well-established *in situ* metalation of 2HTPP molecules by pre- or postdeposition of metal atoms has been studied extensively by STM, scanning tunneling spectroscopy (STS), X-ray photoelectron spectroscopy (XPS) and near edge X-ray absorption fine structure (NEXAFS). In these investigations 2HTPP molecules were metalated with a variety of metals like Co^[63-64], Fe^[65-67], Zn^[68-69], Ce^[70-71] and Ni^[72]. The metalation reaction proceeds either already at RT or in some cases after moderate annealing usually with very high yields.^[11] The aforementioned studies mainly focused on which metal undergoes the metalation reaction and the influence of the order of reactant deposition with the result that in general the metalation reaction on surfaces is rather the rule than an exception.^[11]

However, there is also the possibility to directly introduce metal atoms from the substrate to the porphyrin center. This reaction was referred to as “self-metalation” by Diller et al.^[37] and was first observed by González-Moreno et al. in 2011 for 2H-protoporphyrin IX (2HPPIX) on Cu(110) and Cu(100) at RT.^[23] The reactivity of the substrate plays a significant role as evidenced by further observations of self-metalation of various porphyrins on Cu substrates^[37, 54, 73] as well as recently stated for Fe and Ni substrates.^[74] On the other hand, no self-metalation reactions on rather inert substrates like Ag and Au have been reported up till now. Certainly, 2HTPP on Cu(111) presents an intensively investigated example for the self-metalation of porphyrins.^[11, 37, 39, 75-78] Ditze et al. analyzed in a comprehensive RT STM investigation the metalation rate and the corresponding activation energy of the self-metalation process by Arrhenius analysis at low coverages.^[75] Interestingly, in this process the molecules are not only metalated but the adsorption behavior also changes significantly.^[39] In order to get insight into the mechanism of metal insertion into the porphyrin, DFT calculations have been performed for 2H-porphyrin in the gas phase. The reaction is assumed to take place in three steps: Initially, the metal atom is coordinated to the nitrogen atoms. In the second step the hydrogen atoms are transferred one after the other from the nitrogen atoms to the metal. Finally, H₂ is released from the molecule.^[69]

However, an understanding of the detailed mechanism of the self-metalation reaction as well as control of the latter is certainly still missing. For example Röckert et al. observed in a recent temperature programmed desorption (TPD) study of deuterated 2DTPP that deuterium can be exchanged by hydrogen atoms of the carbon backbone mediated by the surface.^[79] Apparently, different mechanisms as the one proposed by DFT for the gas phase have to be taken into account for the metalation reaction on the surface proving again the active role of the substrate.

Another on-surface reaction of porphyrins to be considered is dehydrogenation.^[39, 78, 80] For 2HTPP on Cu(111) Röckert et al. have shown in a combined STM, TPD and XPS study that annealing to 400 K first leads to the aforementioned self-metalation reaction.^[78] By increasing the annealing temperature to 450 K and 500 K partial loss of hydrogen and the corresponding, intramolecular bond formation between phenyl legs and adjacent pyrrole groups is observed. However, dehydrogenation reactions can also be utilized to link porphyrins to other carbon structures as demonstrated in a study by He et al.^[80] By annealing porphyrin molecules and graphene sheets on a Ag(111) substrate to 620 K, the tetrapyrroles were fused to the graphene edges.

In general, it can be stated that metalation of porphyrins can be observed and is expected at RT or after mild annealing while dehydrogenation proceeds at higher temperatures. Nevertheless, both reaction types are suitable ways to manipulate the properties of porphyrins *in situ*.

4. Results

In this chapter the most important results of the systems investigated in the publications on which the thesis at hand is based on will be discussed. Thereby, common patterns in the adsorption behavior of porphyrins can be deduced giving further insight into fundamental processes and opening up the pathway to tailor the properties of porphyrins on surfaces. A detailed discussion of the individual systems is given in the publications [P1-7] which are attached as appendix.

In more general terms the adsorption behavior of tetraphenylporphyrins on well-defined metal substrates is investigated. To understand the adsorption behavior the complex interplay of molecule-molecule and molecule-substrate interactions has to be determined. However, to draw conclusions about this interplay of interactions the intramolecular conformation of molecules as well as their supramolecular order has to be investigated and described in detail. Figure 4.1 illustrates the relationship of adsorption behavior, intramolecular conformation as well as supramolecular order but also the corresponding points which were specifically investigated and addressed in the thesis at hand.

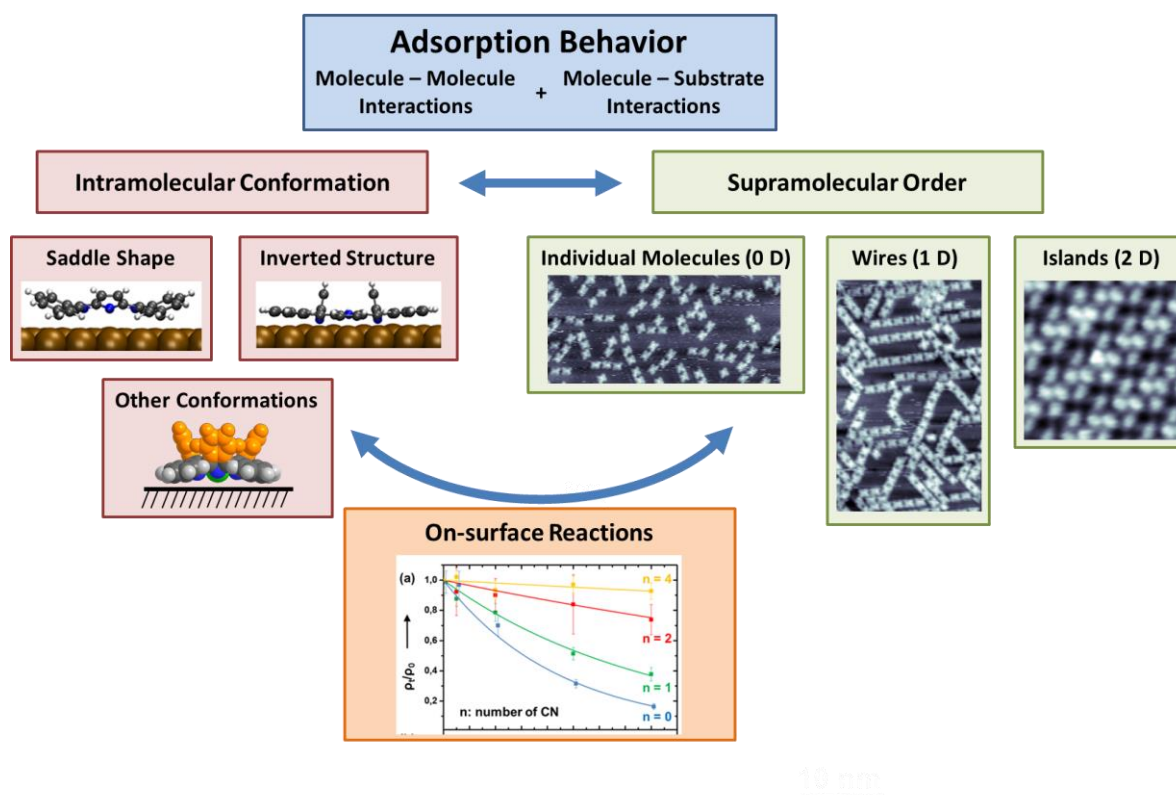


Figure 4.1 Overview scheme illustrating the structure of the discussion of the adsorption behavior in the thesis at hand.

In a first approach the intramolecular conformation of tetraphenylporphyrins will be discussed in respect to the systems investigated in the course of the thesis at hand. As mentioned in the introducing chapters, the intramolecular conformation can be closely linked to the supramolecular order of the respective system. The second main chapter of the results part will therefore be focusing on the supramolecular arrangements which have been found in the course of the thesis at hand. As a third discussion point, on-surface reaction, as well as the influence of porphyrin functionalization on these reactions, will be examined and described. These reactions are of utmost interest since they present ways to *in situ* functionalize the porphyrins and also to modify their adsorption behavior.

4.1 Intramolecular Conformation

The intramolecular conformation of porphyrins is an important part of their adsorption behavior and might allow for conclusions about molecule-substrate and molecule-molecule interactions. As mentioned in the literature review, the adsorption geometry of porphyrins is often described by the so-called “saddle shape” conformation.^[33-36] For a more in-depth discussion of the intramolecular conformation the peculiar adsorption behavior of free-base tetraphenylporphyrin (2HTPP) on Cu(111) needs to be addressed.^[11, 37-38, 48, 50, 52, 75, 81] At low coverages isolated 2HTPPs appear mostly as two elongated parallel protrusions in STM. The individual molecules are oriented and “slowly” diffuse along the three main crystallographic directions at RT.^[38] These observations in STM, which are characteristic for various free-base porphyrins on Cu(111), as well as the corresponding chemical shifts in N 1s X-ray photoelectron spectroscopy (XPS), have been consistently attributed to a strong chemical interaction between iminic nitrogen atoms and Cu substrate.^[37, 39, 77] The molecule is literally pulled towards the surface causing a rather flat adsorption geometry of 2HTPP with the peripheral phenyl rings almost parallel to the substrate. The corresponding intramolecular conformation, referred to as “saddle shape conformation”, as depicted in Figure 4.2 a), has been experimentally deduced from a near edge X-ray adsorption fine structure (NEXAFS) study by Diller et al.^[37] It is not exclusive for 2HTPP but has been proposed for other TPP derivatives on different surfaces as well.^[34-36, 66]

New insights into the adsorption geometry of 2HTPP on Cu(111) have been reported very recently by Albrecht et al. in their atomic force microscopy (AFM) study at low temperatures with a CO-functionalized tip. The AFM measurements suggest an intramolecular

4. Results

conformation with strongly tilted pyrrole groups contradicting the conventional saddle shape. Further evidence and detailed insight in this particular adsorption geometry, referred to as “inverted” conformation, are provided by a combined density functional theory and STM study [P5]. The DFT optimized geometry of both saddle shape and inverted structure of 2HTPP on Cu(111) is presented in Fig 4.2 a) and b).

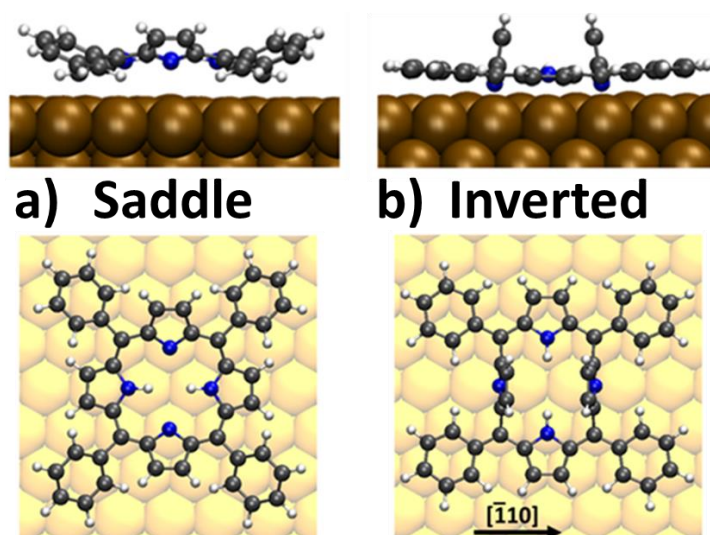


Figure 4.2 DFT optimized geometries of 2HTPP on Cu(111): top and side views of (a) a conventional “saddle-shape” adsorption geometry and (b) an “inverted” adsorption geometry. [modified from P5]

Comparison of the side views in Figure 4.2 a) and b) reveals that, besides the almost perpendicular two pyrrole groups, the inverted structure is almost parallel to the surface in contrast to gas phase and saddle shape geometries. The strong tilt of the two pyrrole rings in the inverted geometry (angle of about 99° with the substrate plane) can be understood by coordination of the corresponding two iminic nitrogen atoms to the Cu(111) surface. Interestingly, DFT calculations for both inverted and saddle shape structure yield that the inverted structure is at least 0.3 eV lower in energy. Due to the peculiar adsorption geometry of the inverted structure a rectangular rather than the square appearance of the saddle shape structure is expected for 2HTPP molecules on Cu(111) in STM. The simulated STM images of the two adsorption geometries, depicted in Fig 4.3 a) (saddle) and b) (inverted), represent the expected different appearance. Initially, the molecular appearance of 2HTPP on Cu(111) was described by two parallel protrusions which does not fit to either of the simulated STM images. The imaging of the two parallel protrusion appearance is most likely caused by a functionalized tip, e.g, by a tip-adsorbed molecule. However, a second predominant

molecular appearance, depicted in Fig 4.3 c), can be found in experiment. Notably, this appearance was independently achieved with three different experimental setups namely with Prof. Abner de Siervo's setup in Campinas (Brazil), Prof. Alexander Schneider's setup and the setup in Erlangen. Several studies from other groups depict this appearance as well but without further discussion.^[33, 48, 50, 73, 81-82]

Intriguingly, the appearance is in very good agreement with the simulated inverted structure. The central protrusions representing the two upright pyrrole rings as well as the rectangular shape strongly suggest the inverted structure instead of the “conventional” saddle shape as adsorption geometry for 2HTPP on Cu(111).

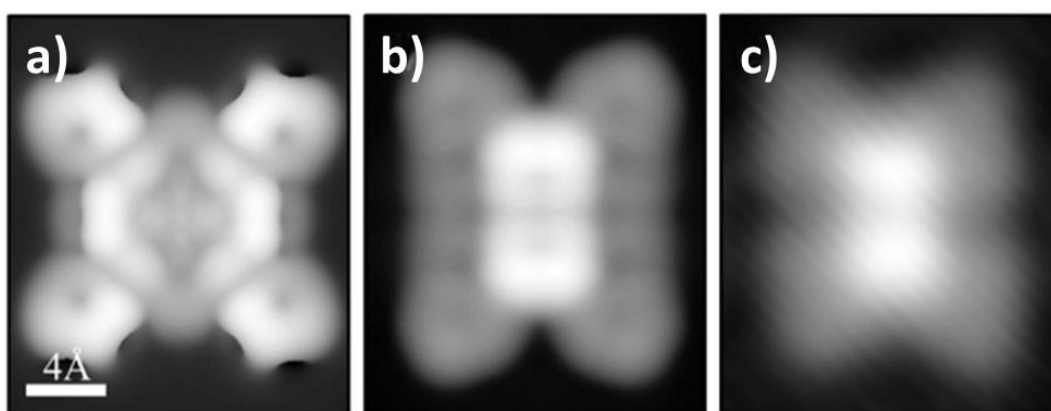


Figure 4.3 DFT simulated geometries of 2HTPP on Cu(111): (a) “saddle-shape” adsorption geometry and (b) “inverted” adsorption geometry. The molecular appearance observed in experiment depicted in (c) is overall rectangular shaped and features two bright, central protrusions. [modified from P5] Tunneling parameters: (a), (b) $U_{\text{bias}} = -1.5 \text{ V}$, $I_{\text{tunnel}} = 30 \text{ pA}$; (c) $U_{\text{bias}} = -1.4 \text{ V}$, $I_{\text{tunnel}} = 37 \text{ pA}$.

Further evidence for the peculiar inverted adsorption geometry can be found by comparing calculated and measured XPS splitting in N1s region as well as X-ray standing wave (XSW) data from literature.^[37, 79, 83] Overall, the comparison yields much better agreement with the inverted than the saddle shape structure underlining the strong interaction of the two iminic nitrogens with the surface.

In addition this novel, inverted structure is also found for the fourfold cyano-functionalized 5,10,15,20-Tetrakis(*para*-cyanophenyl)porphyrin (2HTCNPP) (c.f. Fig 2.3) on Cu(111) and is described in detail in [P5, P6]. For this system the molecular appearance of an individual

4. Results

molecule is rather rectangular and features two bright central protrusions, similar to 2HTPP and the DFT simulated image of the inverted adsorption geometry.

Clearly, the inverted adsorption geometry is closely linked to a strong interaction of iminic nitrogens to the substrate which can be realized for free-base porphyrins on a strongly interacting substrate. However, free-base porphyrins are not necessarily bound to comply the inverted adsorption geometry. On a rather inert surface like Ag(111) a strong, site specific interaction is not expected and therefore also no inverted adsorption geometry. Indeed, for 2HTPP and 2HTCNPP on Ag(111) a molecular appearance is observed which differs significantly from the inverted structure appearance which has been found for both molecules on Cu(111) [P6]. The molecular appearance of 2HTCNPP on Ag(111), shown in Fig 4.4, is rather square and the macrocycle appears with more or less even brightness. Similar results are found for 2HTPP on Ag(111).^[35]

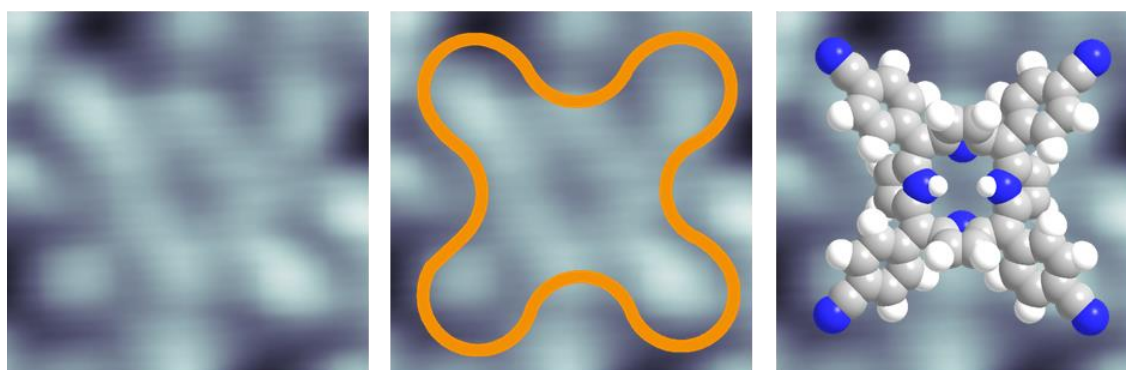


Figure 4.4 Molecular appearance and corresponding intramolecular conformation for 2HTCNPP on Ag(111) at RT. [modified from P6] Tunneling parameters: (a) $U_{\text{bias}} = -31$ mV, $I_{\text{set}} = 26$ pA.

Intuitively, the molecular appearance in this case fits much better with the saddle shape geometry, as depicted in the right part of Fig 4.4. These results underline the role of the substrate for the intramolecular conformation of adsorbed porphyrins.

This relationship of substrate and intramolecular conformation certainly leads to the question how the chemical structure of the porphyrin itself influences the adsorption geometry. For the inverted structure the molecule is almost parallel to the surface with most parts of the molecule within one plane (c.f. Fig 4.2). Therefore, the possibility arises to inhibit the inverted adsorption geometry by introducing steric restrictions within the porphyrin. A novel class of molecules in that regard are certainly tetrabenzoporphyrins, in which four additional

benzene rings are substituted at the β -positions of the macrocycle (c.f. Fig 2.3), presenting steric restrictions directly at the macrocycle. The increased size and spatial requirement of the macrocycle is reflected in the molecular appearance in STM. Fig 4.5 a) illustrates the characteristic molecular appearance of benzoporphyrins featuring two bright, elongated protrusions with a pronounced depression in between [P1, P2 and P4]. While the example in Fig 4.5 a) focuses on Ni(II)-5,10,15,20-tetraphenyltetrabenzoporphyrin (NiTPBP, c.f. Fig 2.3) on Cu(111), i.e., a benzoporphyrin with a metal center, the same molecular appearance is also found for free-base benzoporphyrin species (2HTPBP).

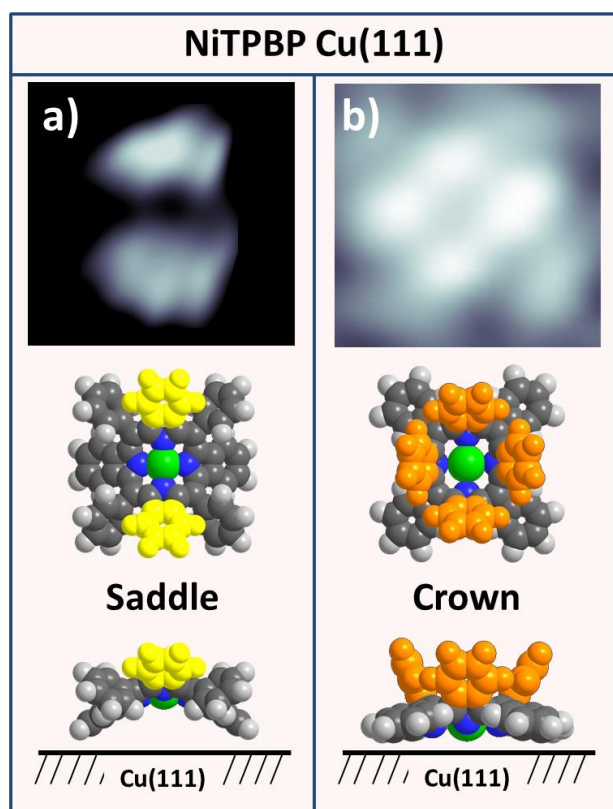


Figure 4.5 Coexisting molecular appearances and corresponding intramolecular conformations for NiTPBP on Cu(111) at RT. The benzopyrrole groups dominating the appearance are colored in yellow and orange, respectively. [modified from P1] Tunneling parameters: (a) $U_{\text{bias}} = 1.31 \text{ V}$, $I_{\text{set}} = 30 \text{ pA}$; (b) $U_{\text{bias}} = -0.59 \text{ V}$, $I_{\text{set}} = 29 \text{ pA}$.

Interestingly, the molecular appearance is largely independent of the bias voltage/polarity. Thus, the observed two bright features are dominated by the topographically highest groups, i.e., two upward bent benzopyrrole groups, marked yellow in the model. By analyzing the distance of the protrusions from the experiment and consulting model DFT gas phase

calculations a saddle shape conformation is deduced, as shown in Fig 4.5 a). Up to now the inverted structure was attributed to a strong molecule-substrate interaction of free-base porphyrin and Cu(111) surface. But for the free-base benzoporphyrin 2HTPBP on Cu(111) a saddle shape geometry is found. The results indicate that by introducing steric restrictions, e.g., via benzopyrrole groups, the overall rather flat inverted structure is hindered.

Besides the saddle shape conformation, NiTPBP on Cu(111) exhibits another co-existing intramolecular conformation as depicted in Fig 4.5 b). The molecular appearance is dominated by four bright protrusions in the center corresponding to four upward bent benzopyrrole groups, colored orange in Fig 4.5 b). The appearance clearly does neither fit with saddle nor inverted structure but corresponds to a peculiar “crown” shape which is stabilized by intermolecular interactions [P1].

So far, the presented results focused on various intramolecular conformations of porphyrins induced by changing either the substrate or the molecule itself. A flexible way to manipulate the intramolecular conformation *in situ* is via on-surface reactions. These reactions can be suitable to trigger a change in the adsorption behavior. Especially self-metalation and dehydrogenation have proven to be important reactions for porphyrins.^[10-11, 60, 78, 80]

The first reaction which should be highlighted here is the stepwise dehydrogenation of Ni(II)-meso-tetrakis(4-tert-butylphenyl)tetrabenzoporphyrin (NiTTBPBP, c.f. Fig 2.3) on a Cu(111) surface after annealing to 400 K [P2]. The reaction sequence can be followed in STM due to a change in molecular appearance as illustrated in Fig 4.6.

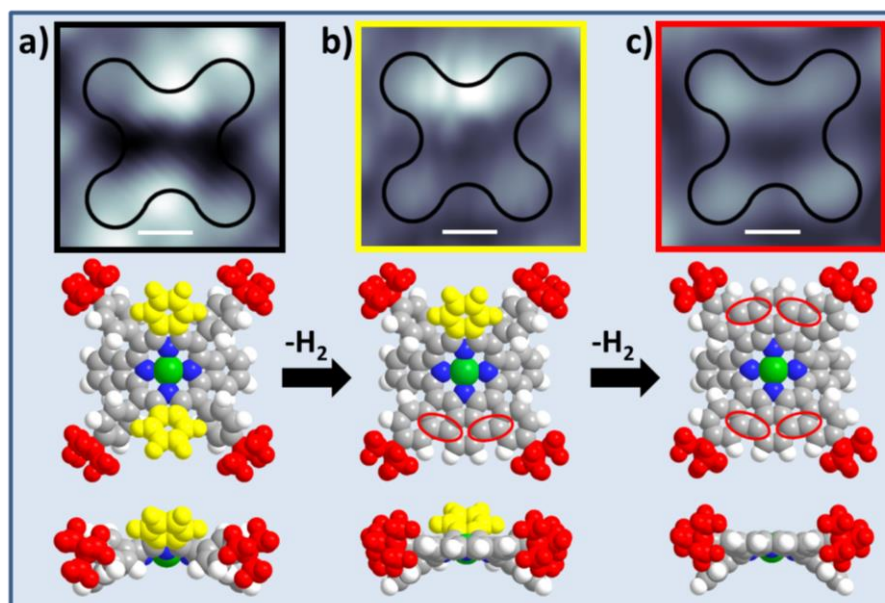


Figure 4.6 Stepwise dehydrogenation of NiTTBPBP on Cu(111) after annealing to 400 K. (a) corresponds to the intact molecule. The red ellipses in (b) and (c) illustrate the new formed C-C bonds. The scale bar is 5 Å. [modified from P2] Tunneling parameters: (a) $U_{\text{bias}} = -1.30$ V, $I_{\text{set}} = 28$ pA; (b) $U_{\text{bias}} = 1.22$ V, $I_{\text{set}} = 27$ pA; (c) $U_{\text{bias}} = 1.22$ V, $I_{\text{set}} = 21$ pA.

Complementary to the aforementioned benzoporphyrins, the high resolution STM image in Fig 4.6 a) depicts the intact Ni-TTBPBP molecule featuring two bright protrusions in the center and four dim protrusions in the periphery. This molecular appearance corresponds to a saddle shape conformation with two upward bent benzene rings (yellow) and four *tert*-butyl groups (red). Annealing the sample to 400 K leads to a different molecular appearance which is depicted in Fig 4.6 b): now only one of the two central, bright protrusions is visible while the peripheral four dim protrusions appear unchanged. This change in appearance is caused by partial dehydrogenation of one of the two upward benzene rings and the neighboring phenyl group. The corresponding C-C bond formation (red ellipses in Fig 4.6) leads to a lowering of the fused benzene ring and thereby to the absence of one of the two central, bright protrusions. Accordingly, in the third motif, depicted in Fig 4.6 c), both halves of the molecule are lowered and thereby no bright central protrusions remain.

Therefore, the dehydrogenation of porphyrins presents a way to fuse the central macrocycle with peripheral groups leading to a change in intramolecular conformation. The intrinsic bond formation limits the flexibility of the porphyrins which potentially causes a significant

change in the adsorption behavior. However, the adsorption behavior of porphyrins can also be directly influenced by modification of the central macrocycle pocket itself. A promising route towards such an *in situ* modification is the self-metalation reaction of tetraphenylporphyrins.^[11, 60] So far, studies were mainly focusing on the reaction of 2HTPP to CuTPP on Cu(111) at 400 K which can be followed in STM and XPS.^[11, 37, 39, 75-78] Up to now the self-metalation reaction has not been reported for porphyrins on rather inert substrates like, e.g., Ag(111). But how is the self-metalation influenced when an open surface like Cu(110), which is considered even more reactive than Cu(111), is used? Interestingly, a study of 2H-tetrakis(3,5-di-tert-butyl)phenylporphyrin (2HTTBPP, c.f. Fig 2.3) on Cu(110) provides evidence for a self-metalation reaction taking place at RT [P3]. The reaction leads to a significant change in molecular appearance and intramolecular conformation as illustrated in Fig 4.7.

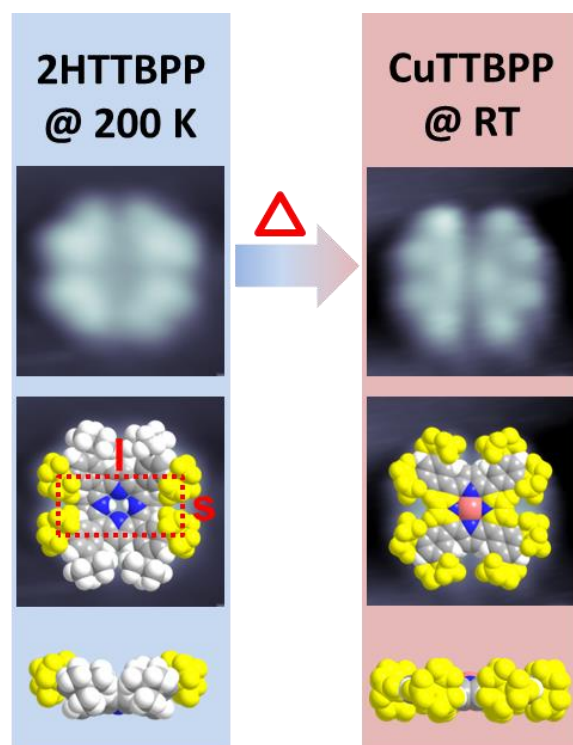


Figure 4.7 Self-metalation of 2HTTBPP to CuTTBPP on Cu(110): At 200 K the free-base porphyrins adsorb as intact molecules. After heating up the substrate to RT the molecules are metalated which leads to a clear change in molecular appearance and intramolecular conformation. [modified from P3] Tunneling parameters: $U_{\text{bias}} = -1.1$ V, $I_{\text{set}} = 30$ pA (left); $U_{\text{bias}} = -1.3$ V, $I_{\text{set}} = 30$ pA (right).

The molecular appearance of 2HTTBPP on Cu(110) at 200 K, depicted in Figure 4.7, resembles a four-fold clover. It is constituted by four paired lobes corresponding to the *tert*-butyl groups of one molecule. By geometric considerations and evaluating the dimensions of the rectangle indicated on the left side of Fig 4.7, the intramolecular conformation can be extracted (for more detail see [P3]).^[31-32] The deduced intramolecular conformation of 2HTTBPP at 200 K resembles a bowl shape. While the periphery is farther away from the surface, the center of the molecule is in close proximity to the substrate which is attributed to strong attractive interactions of iminic nitrogens and Cu substrate. However, this conformation at 200 K is thermally unstable and transforms irreversibly after heating to RT to an appearance dominated by eight equally bright protrusions. The corresponding intramolecular conformation, depicted on the right side of Fig 4.7, lies “flat” on the surface which is attributed to be driven by attractive van der Waals interactions with the substrate. The transformation of the intramolecular conformation from 200 K to RT can be understood by a self-metalation of 2HTTBPP to CuTTBPP upon increasing the sample temperature. Principally, there are further possible explanations for the observed transition beside self-metalation, however these were considered unlikely. A detailed discussion is given in [P3] and in chapter 4.3. Both adsorption geometries depicted in Fig 4.7 resemble neither the aforementioned saddle nor the inverted structure. However, to understand the observed conformations, steric restrictions introduced by the *tert*-butyl groups have to be taken into account which have been reported to lead to unconventional adsorption geometries.^[28, 31, 84] In addition the surface corrugation, especially for an open surface like Cu(110), certainly plays a role for the observed structures. The role of the substrate is underlined by the observation of yet another different molecular appearance and intramolecular conformation of 2HTTBPP adsorbed on the oxygen reconstructed Cu(110) surface [P3]. On Cu(110)-(2x1)O the free-base molecules are also metalated at RT and the corresponding CuTTBPP molecules form two-dimensional arrangements with two different 2D chiralities. Interestingly, the molecular appearance reflects the chirality. Figure 4.8 a) and c) depict the appearance of an individual molecule, one from each chiral domain.

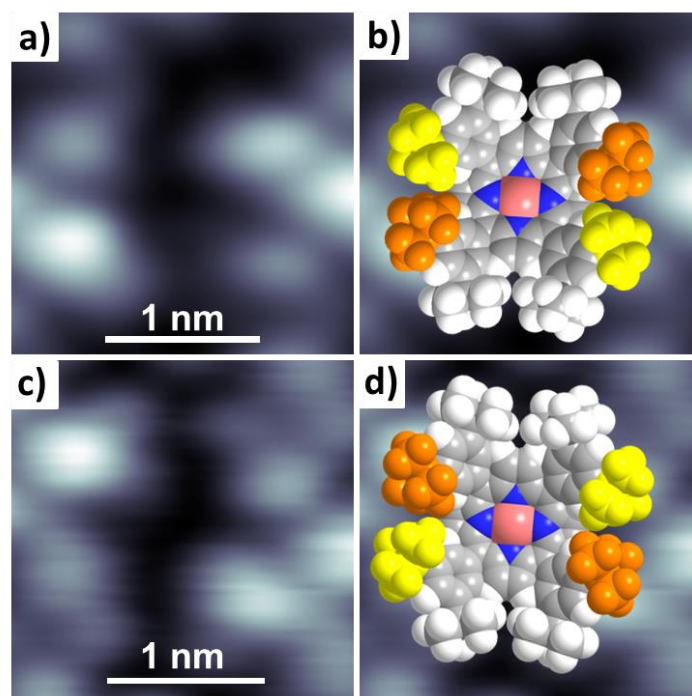


Figure 4.8 Molecular appearance of CuTTBPP on Cu(110)-(2x1)O reflecting the chirality. The orange and yellow colored *tert*-butyl groups in the models correspond to the protrusions observed in STM. [modified from P3] Tunneling parameters: (a) $U_{\text{bias}} = 1.1 \text{ V}$, $I_{\text{set}} = 25 \text{ pA}$; (c) $U_{\text{bias}} = +1.1 \text{ V}$, $I_{\text{set}} = 30 \text{ pA}$.

The molecular appearance in STM is dominated by two bright protrusions and two dimmer protrusions. The corresponding *tert*-butyl groups are marked orange and yellow in the models in Fig 4.8 b) and d), respectively. While the intramolecular conformation resembles a bowl, similar to 2HTBPP at 200 K, a specific deformation assumed to be governed by intramolecular interactions leads to a non-uniform molecular appearance.

The presented results underline that various adsorption geometries can be found for porphyrins adsorbed on metal substrates. These numerous possibilities present a challenge to predict or control the intramolecular conformation and are therefore an important part of the adsorption behavior. However, certain patterns can be distinguished. The novel inverted structure is inherently linked to a strong molecule-substrate interaction of iminic nitrogens and substrate atoms [P5 and P6]. Such an interaction can be realized for free-base porphyrins on substrates with strong site specificity, e.g., like 2HTPP on Cu(111). On rather weak interacting substrates, e.g., on Ag(111), the conventional saddle shape is found. Furthermore, for some free-base porphyrins on Cu(111), the sterically demanding inverted structure is

inhibited and the saddle shape is found. This is the case for the class of tetrabenzoporphyrins in which steric restrictions are introduced to the macrocycle [P1, P2 and P4]. Besides saddle and inverted structure, the flexibility of porphyrin adsorption geometries is further demonstrated by the observation of more complex conformations like crown or bowl-like structures [P1 and P3]. These unconventional structures can be realized by intermolecular stabilization, steric restrictions and/or interactions with open surfaces like Cu(110). Furthermore, self-metalation and dehydrogenation of porphyrins present interesting *in situ* transitions of adsorption geometries which provide the potential to tailor the properties of the adsorbed system [P2 and P3].

4.2 Supramolecular Order

Generally, supramolecular arrangements of different dimensionalities are possible for porphyrins adsorbed on single crystal surfaces. Intrinsically, the lowest possible supramolecular order is 0 (0 D) corresponding to molecules adsorbing as individual, isolated entities. A prominent example for this low ordered state is the intensively investigated 2HTPP on Cu(111) at low coverages.^[37-38, 48, 50, 52, 75-76, 81] At RT, individual, isolated molecules can be observed which are oriented and diffuse “slowly” along the main crystallographic directions of the Cu(111) substrate. There are no indications for attractive interactions in-between the free-base porphyrin molecules. The 2HTPP molecules exhibit an inverted adsorption geometry (c.f. chapter 4.1) due to a molecule-substrate interaction with strong site specificity [P5]. Thus, the molecules are fixed to the densely packed substrate directions and diffuse along these like “trains” on rails.

Similarly, 2HTTBPP (c.f. Fig 2.3) on Cu(110) adsorbed at RT also leads to the observation of individual, isolated molecules which do not form extended self-assembled domains even at coverages close to one monolayer [P3]. Already upon adsorption at RT the strong reactivity of the surface leads to self-metalation of 2HTTBPP to CuTTBPP. In Fig 4.9 an STM image of CuTTBPP on Cu(110) demonstrating the adsorption behavior is shown. The insert depicts the molecular appearance of a single molecule, which has been elaborated before in chapter 4.1.

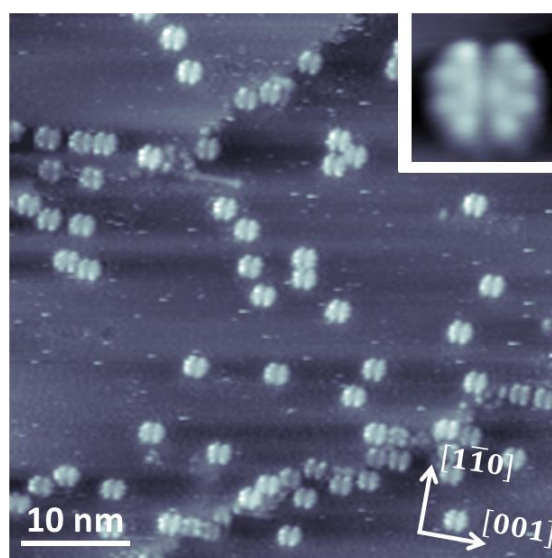


Figure 4.9 STM image of individual, isolated CuTTBPP molecules on Cu(110) with deposition and measurement at RT. The insert depicts a high-resolution image of a single CuTTBPP molecule. [modified from P3] Tunneling parameters: $U_{\text{bias}} = -1.3 \text{ V}$, $I_{\text{set}} = 30 \text{ pA}$.

Interestingly, the molecules are immobile, i.e. no diffusion or rotation is observable at RT. The absence of movement combined with the azimuthal fixation of the molecules to the $[1\bar{1}0]$ direction underlines the strong, attractive, site-specific molecule-substrate interaction. Thus, the adsorption behavior for both 2HTPP on Cu(111) and CuTTBPP on Cu(110) is dominated by strong molecule-substrate interactions which inhibit molecular aggregation and therefore higher supramolecular order.

This correlation offers the potential to modify the adsorption behavior and induce higher supramolecular order by changing the substrate. An easy way to modify the Cu(110) substrate *in situ* is by dosing oxygen and thus creating the (2x1)O reconstructed surface. In contrast to individual, immobile CuTTBPP molecules on the bare substrate, the molecules on the oxygen reconstructed surface are highly mobile and arrange into supramolecular domains [P3]. Figure 4.10 a) and b) depict large scale images of CuTTBPP on the Cu(110)-(2x1)O reconstructed substrate featuring islands with two different 2D chiralities (I and II).

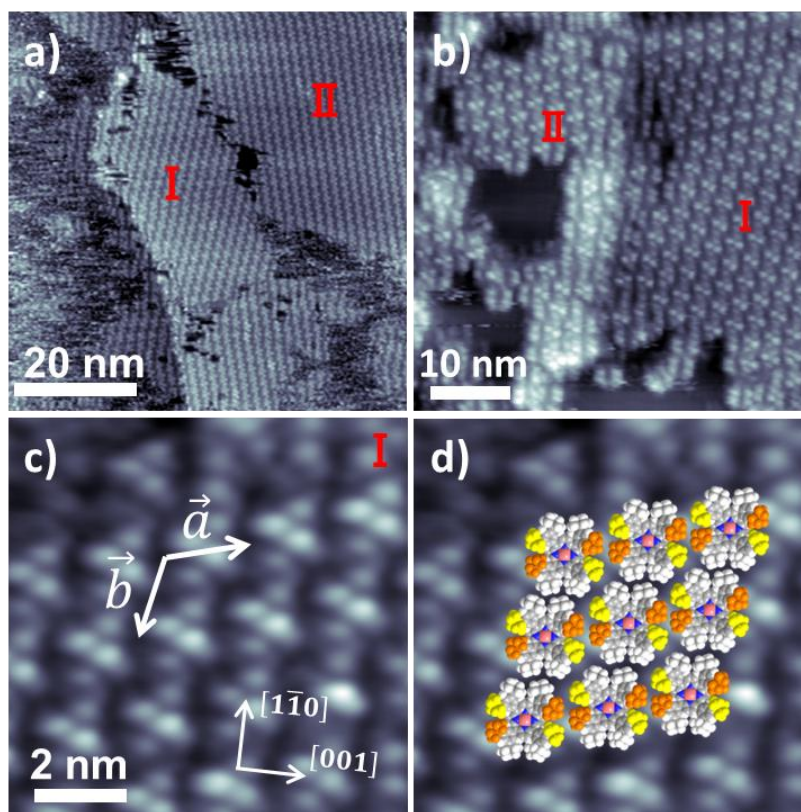


Figure 4.10 (a), (b) overview images of the supramolecular domains found for CuTTBPP on Cu(110)-(2x1)O with two different chiralities (I and II). The hexagonal unit cell is depicted in the zoom-in in (c). The same image is overlaid with molecule models in (d). [modified from P3] Tunneling parameters: (a),(b) $U_{\text{bias}} = -1.1$ V, $I_{\text{set}} = 30$ pA; (c) $U_{\text{bias}} = -1.1$ V, $I_{\text{set}} = 25$ pA.

4. Results

Closer inspection of the molecular arrangement yields a hexagonal unit cell, as depicted in Fig 4.10 c). Based on the molecular arrangement shown in Fig 4.10 d), attractive van der Waals interactions between the *tert*-butyl groups of neighboring molecules are attributed to stabilize the supramolecular structures.^[31, 84] The comparison of the adsorption behavior of CuTTBPP on bare Cu(110) and on the oxygen reconstructed substrate demonstrates that by reducing the molecule-substrate interaction the growth of supramolecular arrangements, stabilized via intermolecular interactions, is promoted.

This naturally leads to the question how the supramolecular order is altered when the molecule-molecule interactions are modified. For self-assembly of molecules cyano groups have certainly demonstrated to be promising side groups by promoting different types of intermolecular interaction motifs.^[56-59] Therefore, in a first approach the functionalization of tetraphenylporphyrins with cyano groups in the periphery will be discussed [P6 and P7]. As depicted in Fig 4.11, the tetraphenylporphyrins are substituted by an increasing number and varying position of cyano groups ($n=1, 2, 4$) at the *para*-positions of the respective phenyl legs for the presented experiments.

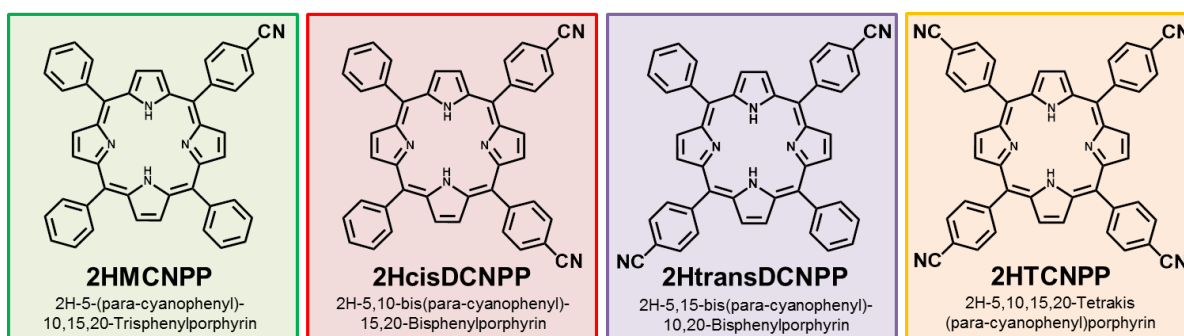


Figure 4.11 Overview of the tetraphenylporphyrins functionalized by an increasing number and varying position of cyano groups ($n=1, 2, 4$) studied in the thesis at hand.

In the following, the single-cyano-functionalized 2H-5-(*para*-cyanophenyl)-10,15,20-Trisphenylporphyrin will be abbreviated with 2HMCNPP („Monocyanoporphyrin“). The double-functionalized 2H-5,10-bis(*para*-cyanophenyl)-15,20-Bisphenylporphyrin with both cyano groups located at adjacent phenyl legs will be referred to as 2HcisDCNPP („Di-cis-cyanoporphyrin“) while the species with two cyano groups located at opposing phenyl legs is addressed as 2HtransDCNPP („Di-trans-cyanoporphyrin“). The fourfold-functionalized 2H-

5,10,15,20-Tetrakis(*para*-cyanophenyl)porphyrin will be abbreviated 2HTCNPP (“Tetracyanoporphyrin”).

The general adsorption behavior of free-base cyanoporphyrins on Cu(111) at RT is quite similar. As an example for the adsorption behavior of cyanoporphyrins on Cu(111), Fig 4.12 a) depicts 2HTCNPP deposited on Cu(111) [P6]. The molecules adsorb as individual entities, and are aligned with respect to densely packed Cu substrate rows. Similar to 2HTPP on Cu(111), the molecular appearance and intramolecular conformation of cyanoporphyrins can be described by the inverted structure caused by a strong molecule-substrate interaction [P5].^[38, 48, 52] While no long-range order is visible, certain arrangements of adjacent cyanoporphyrin pairs, such as illustrated in the zoom-in in Figure 4.12 c), indicate specific intermolecular interactions: The motifs marked with red and blue can be interpreted as due to hydrogen bonds or dipolar couplings respectively, which are known to be typical interaction motifs for cyano linkers.^[56-57, 59, 85-88]

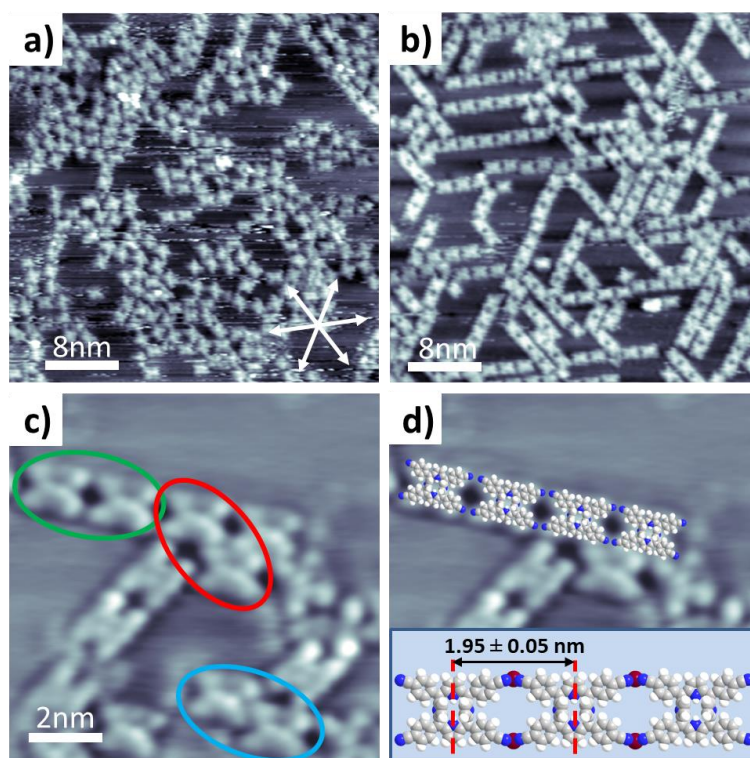


Figure 4.12 STM images of 2HTCNPP on Cu(111) (a) before and (b) after annealing to 400 K for 10 mins. The white arrows mark the crystallographic main directions. In the close-up in (c) the characteristic interaction motifs found for cyanoporphyrins are marked. (d) Superimposed models indicate that the linear motif is facilitated by CN-Cu-CN bonds. [modified from P6] Tunneling parameters: (a) $U_{\text{bias}} = -1.23$ V, $I_{\text{set}} = 27$ pA; (b) $U_{\text{bias}} = -1$ V, $I_{\text{set}} = 27$ pA; (c),(d) $U_{\text{bias}} = -0.90$ V, $I_{\text{set}} = 30$ pA.

Furthermore, a third motif consisting of short 1D multimers, marked in green, can be found. Interestingly, annealing the sample to 400 K for 10 mins, as depicted in Fig 4.12 b), leads to incorporation of the vast majority of 2HTCNPP molecules in 1D multimer chains. Fig 4.12 d) illustrates that the peculiar head-to-head arrangement of cyano groups of neighboring chain molecules in the linear motif can be understood by the linking of two CN groups facilitated by Cu adatoms. A detailed discussion of this metal-organic coordination and the supporting DFT calculations are presented in [P6].

The observation of exclusively linear chains after annealing suggests that the linear motif, which is inherently linked to CN groups and Cu adatoms, is the energetically most stable one for 2HTCNPP. Similarly, molecules arranged in linear motifs are found for the other cyanoporphyrins, respective to the number and position of cyano groups, as depicted in Fig 4.13 [P7]. For 2HMCNPP and 2HcisDCNPP the linear motif is intrinsically limited to two molecules per motif. On the other hand, for 2HtransDCNPP and 2HTCNPP linear chains are found. For 2HtransDCNPP the position of CN groups leads to linking of the molecules in a “zig-zag” fashion within the chains. In general, for all cyanoporphyrins, annealing to 400 K for 10 min leads to incorporation of the majority of molecules in linear arrangements. However, for 2HMCNPP with only one cyano group per molecule, the stabilization in the linear dimer seems to be not favorable enough to be the dominating motif even after annealing. Therefore, the functionalization of tetraphenylporphyrins with CN groups in the periphery presents a pathway to change the supramolecular order of molecules which strongly interact with the substrate from 0D to 1D multimer chains promoted by thermal activation. The observed linear motif presents a novel self-assembled arrangement without any unwanted cross-linking facilitated by the specific alignment of the molecules to the substrate.

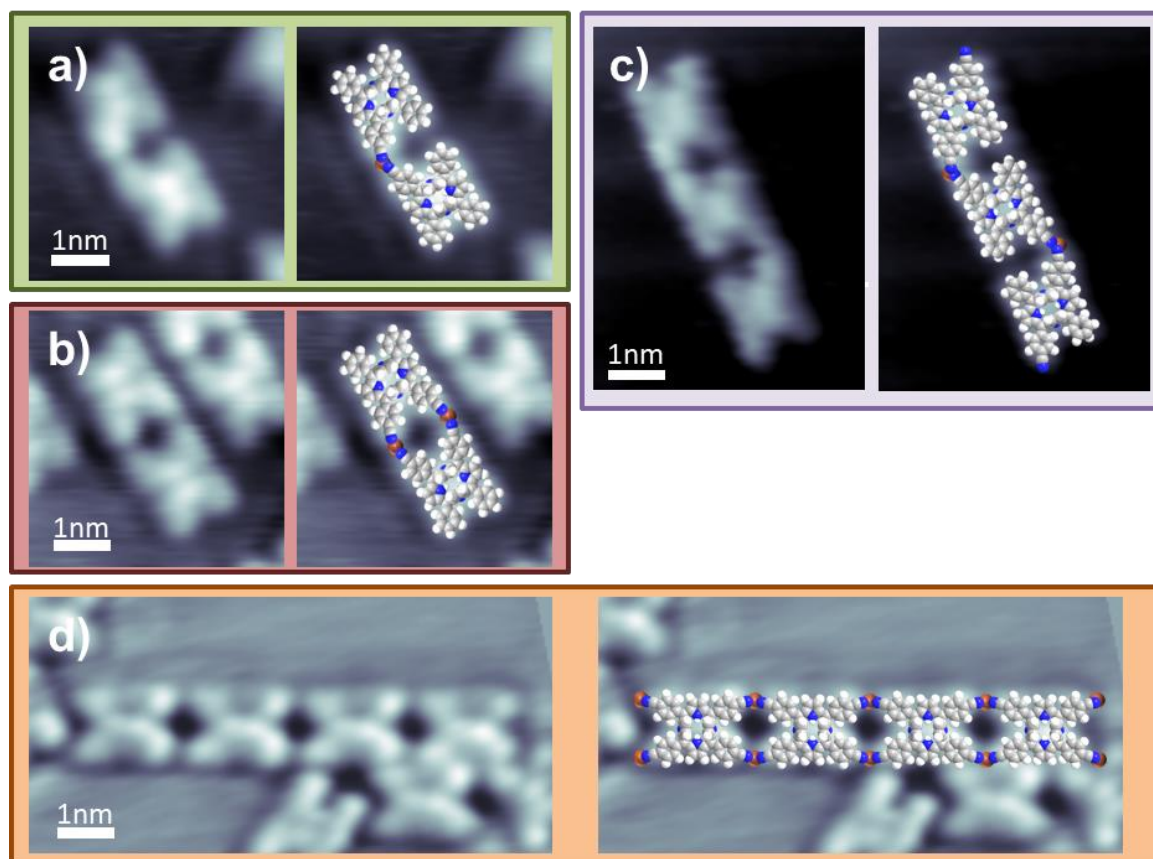


Figure 4.13 Respective to the number and position of cyano groups linear dimers are observed for (a) 2HMCNPP and (b) 2HcisDCNPP, while linear multimers are found for (c) 2HtransDCNPP and (d) 2HTCNPP on Cu(111). [modified from P7] Tunneling Parameters: (a),(d) $U_{\text{bias}} = -0.90$ V, $I_{\text{set}} = 30$ pA; (b) $U_{\text{bias}} = -1.22$ V, $I_{\text{set}} = 30$ pA (c) $U_{\text{bias}} = -1$ V, $I_{\text{set}} = 26$ pA.

So far, the presented results have demonstrated that the strong molecule-substrate interaction of free-base porphyrins which limits supramolecular arrangements was lifted by changing the substrate or was overcome by strong metal-organic coordination bonds. However, the question remains if the limiting, strong molecule-substrate interaction can be lifted by introducing steric restrictions in the molecular structure. As described in chapter 4.1, the inverted structure which is inherently linked to a strong, site specific interaction of free-base porphyrins on Cu(111) is inhibited by substitution of benzene rings to the pyrrole groups of the macrocycle. Thus, in a next step the adsorption behavior of 2H-5,10,15,20-tetraphenyltetrabenzoporphyrin (2HTPB) on different substrates will be discussed [P4]. Fig 4.14 presents an overview of the observed supramolecular arrangements of 2HTPB on the investigated substrates.

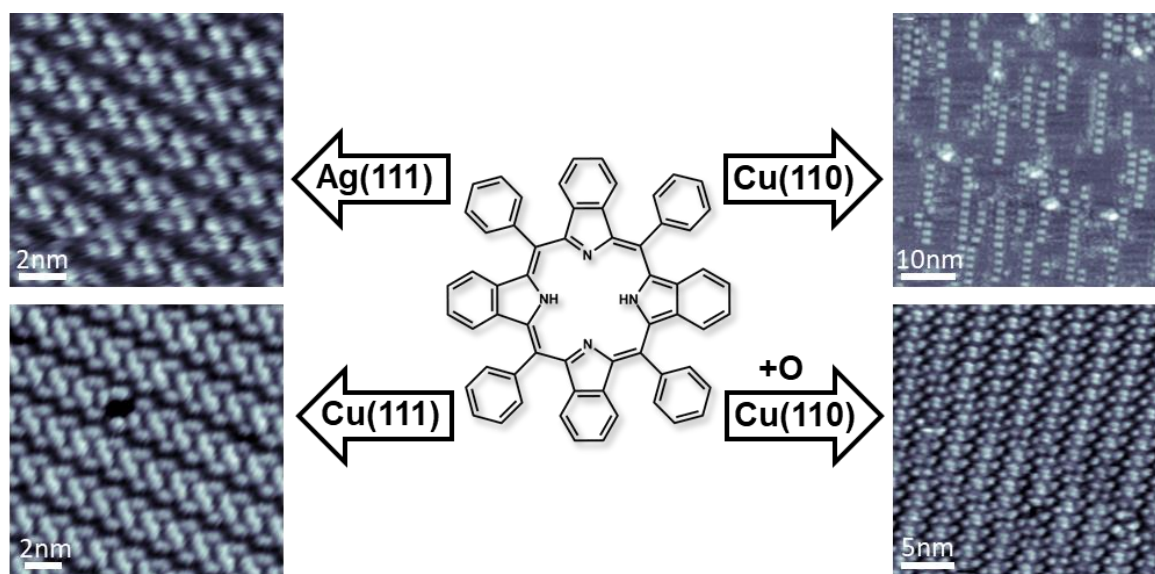


Figure 4.14 Overview of the adsorption behavior of 2HTPB on different surfaces at RT. [modified from P4] Tunneling parameters: $U_{\text{bias}} = 1.20 \text{ V}$, $I_{\text{set}} = 30 \text{ pA}$ (left top); $U_{\text{bias}} = 1.08 \text{ V}$, $I_{\text{set}} = 30 \text{ pA}$ (left bottom); $U_{\text{bias}} = 1 \text{ V}$, $I_{\text{set}} = 30 \text{ pA}$ (right top); $U_{\text{bias}} = -1.08 \text{ V}$, $I_{\text{set}} = 30 \text{ pA}$ (right bottom).

On Cu(111), Ag(111) as well as on the oxygen reconstructed Cu(110) surface the 2HTPB molecules are able to diffuse and form 2D aggregates at sufficient intermolecular stabilization at RT. The observed 2D supramolecular domains exhibit a herringbone arrangement which appears to be characteristic for benzoporphyrins. No individual molecules are observed; thus, the additional benzene rings indeed inhibit interaction with the surface and molecule-molecule interactions govern the adsorption behavior.

In order to understand the herringbone arrangement the molecular arrangement and intermolecular interactions will be discussed for the case of 2HTPB on Ag(111), as depicted in Fig 4.15. The ellipses in Fig 4.15 b) indicate that the molecules, similar to other benzoporphyrins, appear as two bright protrusions corresponding to two upright benzopyrrole groups (c.f. chapter 4.1), colored yellow in Fig 4.15 c). In the structure in Fig 4.15 b), the protrusions are arranged in a way that wider brighter rows (composed of a dense grouping of protrusions) are separated by narrower darker rows. From the superimposed models in Fig 4.15 c) it can be derived that the molecules are oriented such that the upward bent benzene rings of dark row molecules face the downward bent benzene rings of neighboring bright row molecules (indicated by two black bars). This orientation and the distance between groups strongly suggest π - π stacking interactions which stabilize and induce the herringbone

arrangement.^[51] Further stabilization by T-type (indicated by the green solid lines forming a chevron) and attractive van der Waals interactions (indicated by green dashed lines) is proposed.

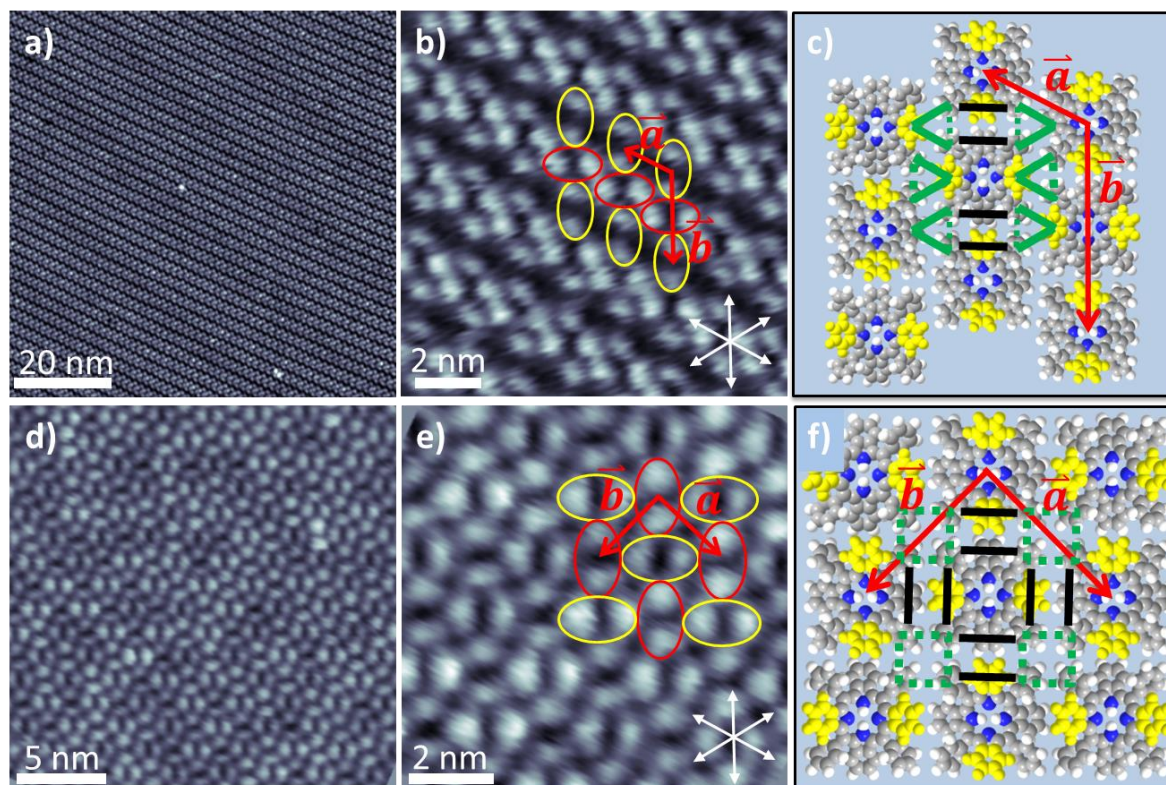


Figure 4.15 (a) STM image of the supramolecular structure formed by 2HTPBPs on Ag(111) at RT. (b) Zoom-in of the herringbone structure. The individual molecules with different orientations are highlighted by the colored ovals. (c) Structural model of the molecular arrangement. The π - π stacking interactions are indicated by black parallel lines. The T-type and van der Waals interactions are marked with solid and dashed green lines, respectively. (d) STM image after annealing 2HTPBPs on Ag(111) to 500 K for 10 min. (e) Zoom-in of the structure featuring a square unit cell. (f) Structural model of the molecular arrangement indicating the relevant intermolecular interactions. [modified from P4] Tunneling parameters: (a) $U_{\text{bias}} = 1.0$ V, $I_{\text{set}} = 30$ pA; (b) $U_{\text{bias}} = 1.2$ V, $I_{\text{set}} = 30$ pA; (d),(e) $U_{\text{bias}} = 1.0$ V, $I_{\text{set}} = 30$ pA.

The importance of this π - π stacking interaction of benzopyrrole groups for the supramolecular arrangements of benzoporphyrins is solidified by annealing experiments. After annealing 2HTPBPs on Ag(111) to 500 K for 10 min, as depicted in Fig 4.15 d) and e), the hexagonal supramolecular structure is not observed anymore, but instead large area domains with a square unit cell are found. While the molecular appearance is unchanged, the

molecular arrangement within the square structure in Fig 4.15 f) illustrates that now all four benzene rings in each molecule display π - π stacking interactions with one benzene ring in the neighboring molecule. That means that the number of such interactions is doubled in the square arrangement compared to the hexagonal structure before annealing. The formation of square order is apparently kinetically hindered at RT, but the corresponding activation barriers can be overcome by the applied heating procedure.

The herringbone arrangement caused by π - π stacking interactions is also found for 2HTPBP on Cu(111) (c.f. Fig 4.11). However, on Cu(111) a coverage dependency of the herringbone arrangement is observed. A detailed explanation and discussion can be found in [P4].

A significant change of supramolecular order from 2D to 1D structures can be observed for deposition of 2HTPBP on the strongly corrugated Cu(110) surface. Fig 4.14 depicts that 1D linear chains of 2HTPBP molecules along the $[1\bar{1}0]$ direction are observed. These chains are stabilized by the downward bent benzo groups which are located in the troughs in $[1\bar{1}0]$ direction establishing an attractive interaction with the substrate. On the other hand, for 2HTPBP on the oxygen reconstructed Cu(110) surface, the strong molecule-substrate interaction is lifted again and a 2D supramolecular arrangement is found (c.f. Fig 4.14).

The presented results of 2HTPBP on Cu(111) and Ag(111) demonstrate that by benzene substitution to the pyrrole groups steric restrictions are introduced in the molecular structure which influence the intramolecular conformation and, thus, inhibit strong molecule-substrate interactions. Therefore, the adsorption behavior is mainly determined by molecule-molecule interactions leading to observation of herringbone arrangements promoted by π - π stacking interactions of benzopyrrole groups.

The results discussed above highlight the influence on the adsorption behavior by functionalization of the β -positions macrocycle. But how is the adsorption behavior modified when the macrocycle center or the periphery of benzoporphyrins is functionalized? Intriguingly, by adding a Ni atom to the center of 2HTPBP a wealth of three different, coexisting supramolecular arrangements, as depicted in Fig 4.16, can be observed for NiTBPP on Cu(111) at RT [P1]. The coexistence of oblique (I), herringbone (II) and cross (III) arrangement suggests that each structure presents a local energetical minimum. However, after annealing only the herringbone structure remains indicating that the latter is the energetically most favorable one.

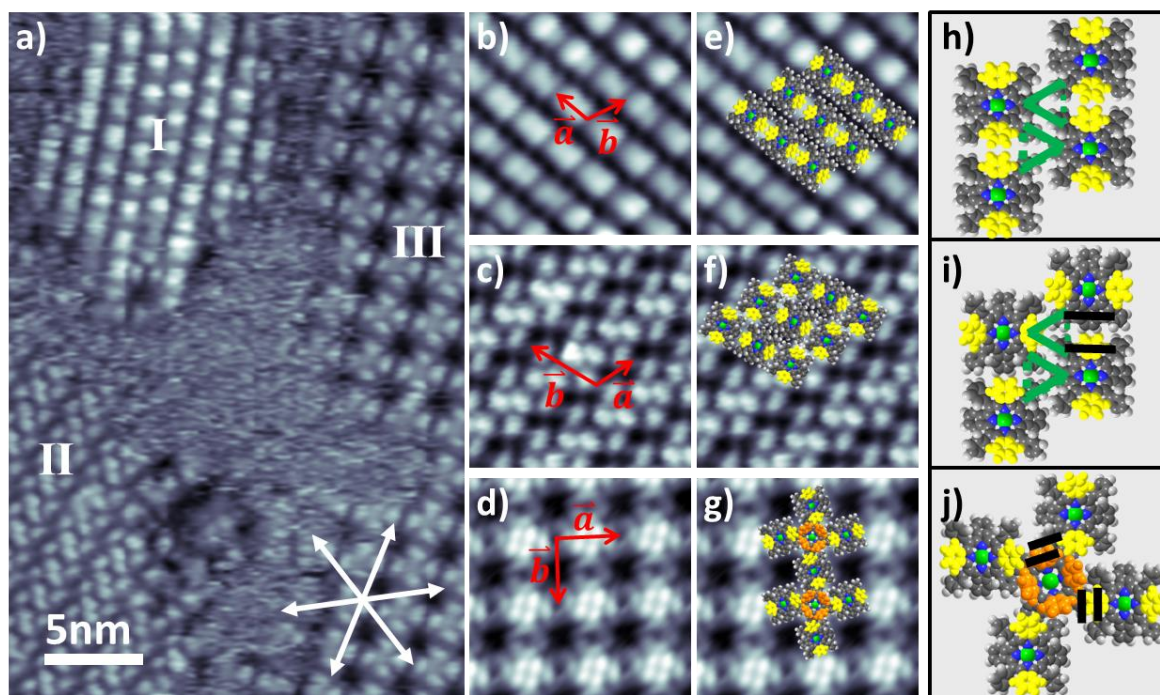


Figure 4.16 (a) STM image of NiTPBP on Cu(111) at RT. Three supramolecular arrangements coexist: I: oblique, II: herringbone, III: cross structure. The white arrows indicate the close packed substrate directions. (b-d) high resolution STM images depicting the individual arrangements. The molecular arrangement in the islands is derived by superimposing the molecular models (e-g). The relevant intermolecular interactions for the three arrangements are shown in (h-j). While π - π interactions are marked by black parallel lines, T-type and van der Waals interactions are indicated by green solid and dashed lines, respectively. [modified from P1] Tunneling parameters: (a-c) $U_{\text{bias}} = 1.31$ V, $I_{\text{set}} = 30$ pA; (d) $U_{\text{bias}} = -0.59$ V, $I_{\text{set}} = 29$ pA

The NiTPBP molecules in the domains appear as two bright protrusions corresponding to two upward bent benzopyrrole groups, similar to the free-base species discussed before. Another similarity to 2HTPBP, is the energetically favorable herringbone arrangement (II), depicted in Fig 4.16 c), f) and i), which is mainly stabilized by the characteristic π - π stacking interactions of benzopyrrole groups, marked with black lines in i). On the other hand, in the oblique structure (I), depicted in Fig 4.16 b), e) and h), all molecules are oriented the same; thus, no π - π stacking interactions of benzopyrrole groups can be established. The structure is only stabilized by rather weak and insufficient T-type and van der Waals interactions, indicated green in h). The peculiar cross structure, depicted in Fig 4.16 d), g) and j), is build up by two types of molecules: “bridging” molecules corresponding to the saddle shape conformation and “center” molecules exhibiting a crown-like conformation. Stabilization of

4. Results

the cross-like structure is mainly facilitated by π - π stacking interactions of the four upward bent benzopyrrole groups of a center molecule and the peripheral phenyl rings of the adjacent bridging molecules. All in all, the observed polymorphism of NiTPBP on Cu(111) is attributed to a subtle balance between different intermolecular and molecule-substrate interactions.

The results of 2HTBPP and NiTPBP highlight the importance of the characteristic π - π stacking interactions of benzopyrrole groups. But can these interactions be inhibited by peripheral functionalization with sterically demanding groups and how does it affect the adsorption behavior?

Therefore, the adsorption behavior of NiTPBP functionalized with bulky *tert*-butyl groups at the *para*-positions of each phenyl leg will be discussed. Fig 4.17 depicts that Ni(II)-meso-tetrakis (4-*tert*-butylphenyl) tetrabenzoporphyrin (NiTTBPBP) molecules on Cu(111) self-assemble to 2D long-range ordered islands with a square lattice [P1 and P2].

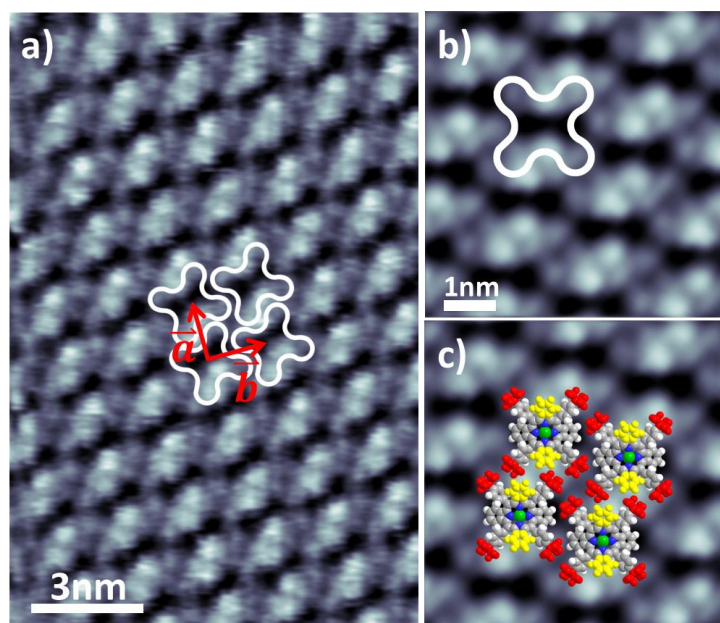


Figure 4.17 (a) STM image of the supramolecular arrangement with a square unit cell observed for NiTTBPBP on Cu(111). The position and orientation of molecules is illustrated by the white molecular shapes. (b) Magnified and rotated image of a supramolecular domain. (c) The micrograph from (b) superimposed with molecular models. [modified from P1] Tunneling parameters: (a–c) $U_{\text{bias}} = -1.30$ V, $I_{\text{set}} = 28$ pA.

The molecular appearance is constituted by two central bright protrusions according to benzopyrrole groups and four dim protrusions corresponding to four upper *tert*-butyl groups. The molecular arrangement illustrated in Fig 4.17 c) suggests stabilization via van der Waals interactions. Apparently, the functionalization with *tert*-butyl groups does indeed hinder π - π stacking interactions of benzopyrrole groups by increasing the steric demand in the periphery of the molecules; thus, no herringbone arrangement of molecules is observed.

In conclusion, the adsorption behavior of porphyrins and their different supramolecular order is linked to several factors. Molecules which interact strongly with the surface exhibit limited or no diffusion corresponding to the observation of isolated molecules and the absence of supramolecular order [P3 and P5]. However, one dimensional order can be established for tetraphenylporphyrins exhibiting strong molecule-substrate interaction by functionalization with CN groups establishing CN-Cu-CN coordination which is promoted by thermal treatment [P6 and P7]. To increase the supramolecular order even further, the strong molecule-substrate interaction has to be reduced. This can be achieved by either introducing steric restrictions within the molecule, e.g., by attaching benzene rings to the pyrrole groups, or by modifying the substrate itself, e.g., by formation of an oxygen reconstructed Cu(110) substrate [P1-4]. Thereby, the molecules are able to diffuse freely on the substrate and arrange into supramolecular arrangements stabilized by intermolecular interactions. The detailed arrangement of molecules within these domains is determined by a complex interplay of molecule-molecule and molecule-substrate interactions. Peripheral functionalization of the porphyrins can further modify the 2D arrangements of molecules yielding potential control of these self-assembled structures. For example functionalization of the peripheral phenyl legs with sterically demanding *tert*-butyl groups inhibits aromatic interactions resulting in the observation of novel supramolecular domains for benzoporphyrins.

4.3 On-Surface Reactions

In this chapter the evaluation of on-surface reactions of tetraphenylporphyrins, namely self-metalation and dehydrogenation, will be discussed. On-surface reactions present a flexible approach towards *in situ* modification of the adsorption behavior. Especially, self-metalation has been the most relevant *in situ* reaction for free-base porphyrins in literature.^[10-11, 60] The focal point of these studies was the self-metalation reaction of 2HTPP on Cu(111) to CuTPP which can be followed by STM, TPD and XPS.^[37, 39, 77] However, in these studies it was not addressed how to selectively influence or even control the self-metalation rate of free-base porphyrins.

So far, the discussed results have demonstrated that the adsorption behavior of tetraphenylporphyrins is closely linked to their peripheral functionalization. This raises the question if the self-metalation rate can be modified when the phenyl legs are functionalized. Therefore, the self-metalation behavior of cyanoporphyrins on Cu(111) compared to the one of 2HTPP will be discussed at this point [P7]. Annealing cyanoporphyrins on Cu(111) to 400 K for 10 mins promotes the formation of linear arrangement of molecules facilitated by CN-Cu-CN linking. Different kinds of linear multimers were found respective to the number and position of CN groups within the molecules (c.f. chapter 4.2). However, at closer inspection it can be found that for extended annealing to 400 K the formation of linear arrangements is accompanied by an overall decrease of the number of free-base species and observation of stripy features in STM. Fig 4.18 depicts a series of STM images for the single-cyano-functionalized 2HMCNPP after different heating times at 400 K. The decrease of free-base species after heating is strongest for 2HMCNPP and becomes less pronounced with increasing number of CN groups.

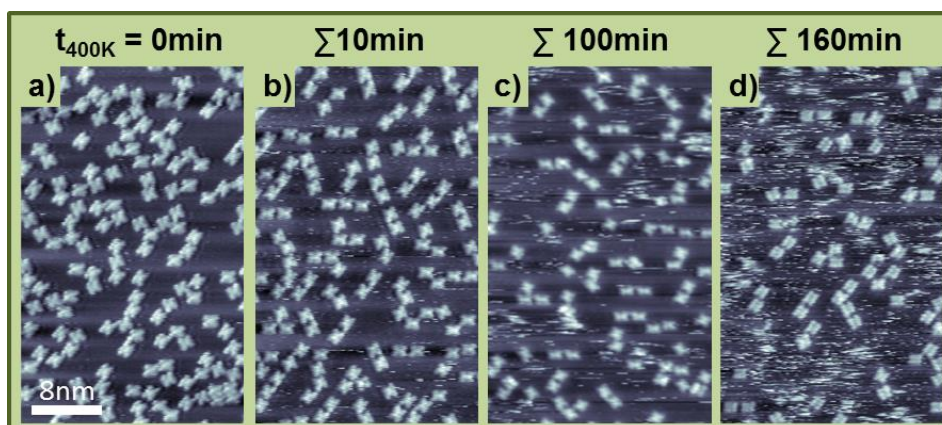


Figure 4.18 Series of STM images of 2HMCNPP at RT after annealing to 400 K for indicated times. The heating induces a decrease of the number of individual molecules on the structure accompanied by observation of stripy features. This so-called 2D gas phase can be explained by mobile CuMCNPP molecules. [modified from P7] Tunneling parameters: (a) $U_{\text{bias}} = -226 \text{ mV}$, $I_{\text{set}} = 31 \text{ pA}$; (b) $U_{\text{bias}} = -0.88 \text{ V}$, $I_{\text{set}} = 30 \text{ pA}$; (c) $U_{\text{bias}} = -1.35 \text{ V}$, $I_{\text{set}} = 29 \text{ pA}$; (d) $U_{\text{bias}} = -0.97 \text{ V}$, $I_{\text{set}} = 30 \text{ pA}$.

The observation of stripy features is attributed to fast diffusing molecules, also referred to as 2D gas phase.^[52] This change in adsorption behavior, reported for annealing of 2HTPP on Cu(111) as well, can be understood by a self-metalation reaction of free-base species to their respective Cu-cyanoporphyrin equivalents.^[37, 39, 78] Due to the binding of a metal center the strong, attractive interaction of porphyrin macrocycle and Cu substrate cannot be established anymore. The metalated molecules literally “pop up” from the surface and become more mobile.^[75, 84]

In order to get further insight into the self-metalation reaction for cyanoporphyrins and to compare it to the one of the well-investigated 2HTPP, the remaining individual free-base porphyrins after each annealing step for 2HMCNPP ($n = 1$), 2HcisDCNPP ($n = 2$) and 2HTCNPP ($n = 4$) have been counted (with n being the number of CN groups). By plotting the corresponding data versus time on a linear and on a logarithmic scale, as depicted in Fig 4.19 a) and b) respectively, the self-metalation rate can be determined.^[75]

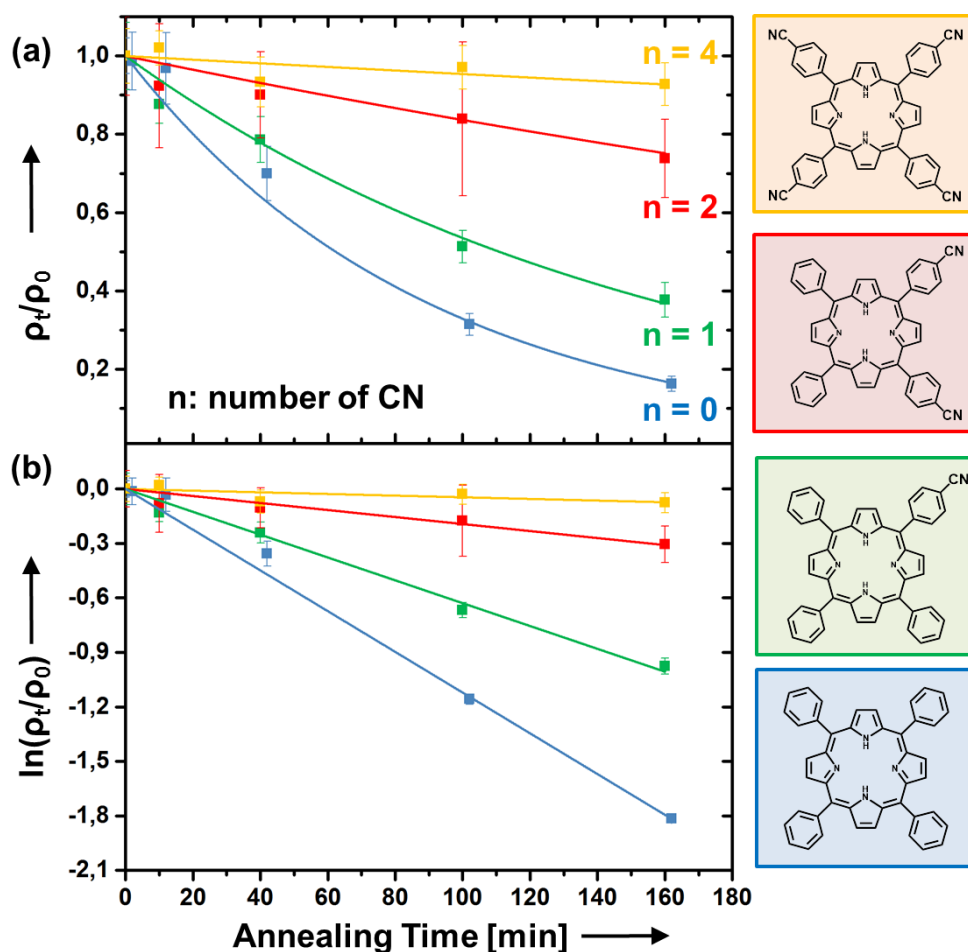


Figure 4.19 Graphs with (a) linear and (b) logarithmic scale demonstrating the development of normalized free-base porphyrin (reactant) coverage with the annealing time at 400 K. The data sets of 2HMCNPP (green), 2HcisDCNPP (red), 2HTCNPP (orange) and 2HTPP (blue) are shown. [modified from P7]

The very good agreement of the fits for each porphyrin including an exponential decay curve indicates a pseudo-first-order reaction behavior for all 2H-cyanoporphyrins and for 2HTPP. Interestingly, the data reveals a pronounced trend towards lower self-metalation rates by introducing more cyano groups per tetraphenylporphyrin molecule; thus presenting an interesting tool for the tailoring of molecular properties. A detailed explanation for the reduced self-metalation rates has yet to be found; however, the trend is certainly linked to the inverted structure as well as an electronic influence of the CN groups, and possibly to the lowered mobility and higher stability of reactants due to fixation in linear multimers.

The modification of the self-metalation rate presents a significant step towards the controlled fabrication of nanostructures and their reactions. As a second determining parameter for self-metalation, the reaction temperature has to be considered. So far, the self-metalation of the presented free-base porphyrins on Cu(111) has been reported to proceed with significant yield at 400 K.^[75, 84] However, the reaction may already take place at RT when an open surface like Cu(110) is used.^[23] Fig 4.20 illustrates the self-metalation reaction and the corresponding change in molecular appearance and intramolecular conformation of 2HTTBPP on Cu(110) [P3]. At 200 K the free-base species, depicted on the left side of Fig 4.20, is intact. After heating the substrate to RT, the molecules irreversibly transfer to the situation depicted in the middle part of Fig 4.20 which is attributed to the self-metalation reaction forming CuTTBPP.

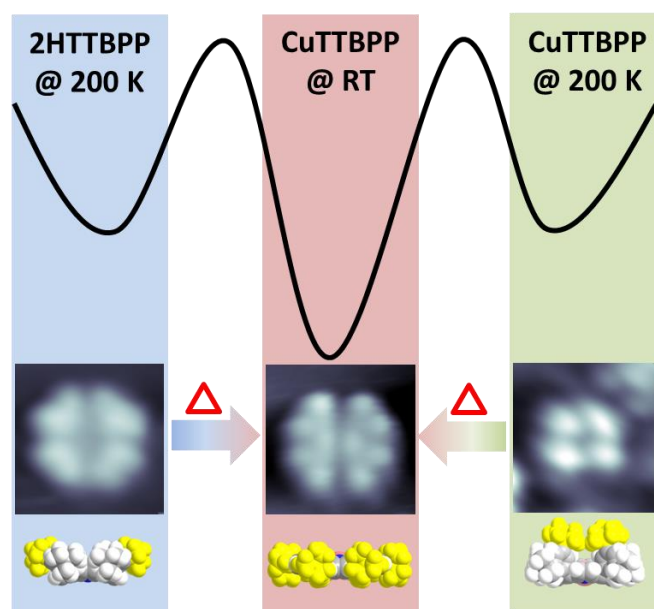


Figure 4.20 Schematic illustration of the energy scheme for 2HTTBPP and CuTTBPP on Cu(110) surfaces at 200 K and RT. At RT the 2HTTBPP molecules react with the substrate copper atoms and form CuTTBPP molecules. The self-metalation reaction is traceable by the change in molecular appearance and intramolecular conformation. [modified from P3] Tunneling parameters: $U_{\text{bias}} = -1.1$ V, $I_{\text{set}} = 30$ pA (left); $U_{\text{bias}} = -1.3$ V, $I_{\text{set}} = 30$ pA (middle); $U_{\text{bias}} = -1.0$ V, $I_{\text{set}} = 29$ pA (right).

In order to rule out other possible explanations for the observed change in molecular appearance like dehydrogenation or activated transition toward a more stable conformation, the metalated version, CuTTBPP, is investigated at 200 K and RT. Comparing the adsorption geometries in Fig 4.20 demonstrates that despite their very different intramolecular

conformations at 200 K, 2HTTBPP and CuTTBPP transform into the same conformation at RT. These observations are a strong indication that 2HTTBPP molecules indeed self-metalate with Cu substrate atoms to form CuTTBPP at RT. The irreversible change of the intramolecular conformation of CuTTBPP from 200 K to RT is a result of the additional thermal energy at RT which is sufficient to overcome steric hindrance within the molecule. The observation of lower self-metalation temperature of free-base porphyrins on an open surface can be tentatively explained by the much higher number of copper adatoms on Cu(110) compared to Cu(111).^[23, 37, 89]

On-surface reactions of tetraphenylporphyrins are not solely limited to *in situ* functionalization of the macrocycle center with metals. Chemical modification can also be induced in the periphery of the molecules. Röckert et al. demonstrated that at elevated temperatures on Cu(111) the self-metalation reaction of 2HTPP to CuTPP is followed by partial dehydrogenation.^[39, 78] Thereby, C-H bonds from pyrrole groups and peripheral phenyl rings are cleaved and H₂ is released while new C-C bonds are formed. This intramolecular reaction is inherently interesting for the adsorption behavior of benzoporphyrins for which the central benzopyrrole groups have proven to play a significant role (c.f. chapter 4.2). Fig 4.21 depicts STM images of Ni(II)-meso-tetrakis(4-tert-butylphenyl)tetrabenzoporphyrin (NiTTBPBP) on Cu(111) for high coverage, i.e., close to 1 monolayer (Fig 4.21 a) and b)), and lower coverage (Fig 4.21 c) and d)) after annealing to 400 K [P2]. The insert in Fig 4.21 b) illustrates that after heating three coexisting motifs/appearances can be distinguished. As described in chapter 4.1, the change in molecular appearance is correlated to a stepwise partial dehydrogenation. The reaction sequence and the respective motifs are illustrated in the right part of Fig 4.21: motif 1 corresponds to the intact molecules (marked black), motif 2 is the species after the first partial dehydrogenation step (marked yellow) and motif 3 is the species after the second and final dehydrogenation step (marked red). If the sample is heated further to 450 K (not shown), practically all molecules exhibit the red motif which confirms that the yellow motif is an intermediate state.

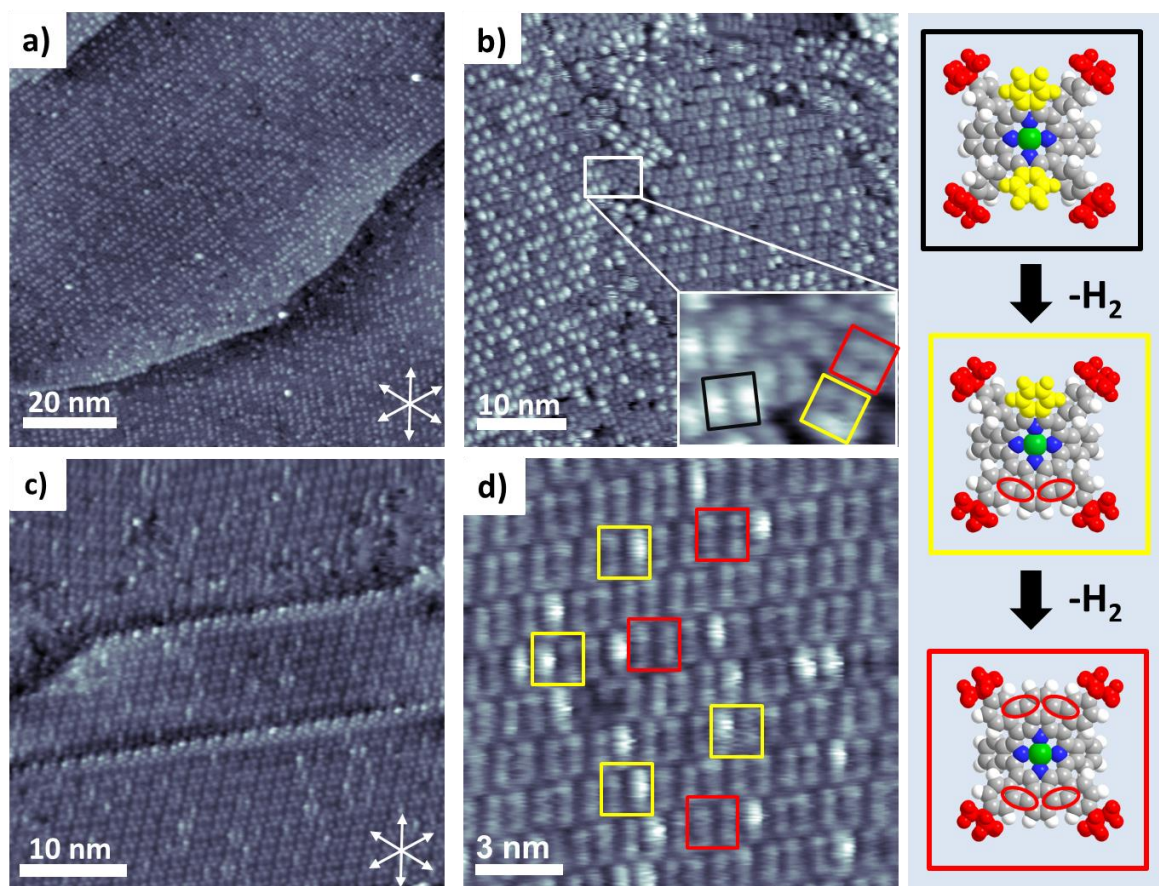


Figure 4.21 (a) and (b) STM images after annealing NiTTBPBP on Cu(111) at 400 K for 10 min for a coverage close to 1 monolayer ($\theta = 0.022$ ML). (c) and (d) STM images after the same annealing procedure but for lower coverage ($\theta = 0.013$ ML). Images (c) and (d) were imaged at 200 K because of the higher mobility compared to the 0.022 ML coverage. The colored squares in (b) and (d) highlight the three motifs corresponding to the partial dehydrogenation depicted on the right side. [modified from P2] Tunneling parameters: (a),(b) $U_{\text{bias}} = -1.18$ V, $I_{\text{set}} = 21$ pA; (c) $U_{\text{bias}} = 0.99$ V, $I_{\text{set}} = 27$ pA; (d) $U_{\text{bias}} = 0.99$ V, $I_{\text{set}} = 28$ pA.

On the other hand, in Fig 4.21 c) and d) STM images for lower NiTTBPBP coverage but the same annealing procedure (10 mins at 400 K) are depicted. Interestingly, the number of modified appearances, that is yellow and red motif, in Fig 4.21 a) and c), is significantly larger for lower coverage (Fig 4.21 c)). This trend is highlighted by table 1 which summarizes a statistical analysis of the different motifs achieved at different annealing temperatures (400 and 450 K for 10 min) and initial coverages.

Table 1. Occurrence of the different motifs in percent (%), for different initial coverages (θ) after annealing for 10 min at different temperatures.

	Annealing Temperature			
	400 K Lower coverage ($\theta = 0.013$ ML)	400 K High coverage ($\theta = 0.022$ ML)	450 K Lower coverage ($\theta = 0.013$ ML)	450 K High coverage ($\theta = 0.022$ ML)
Motif 1	0.5±0.4%	17.1±1.9%	0%	0%
Motif 2	12.3±3.2%	42.0±5.1%	1.7±0.9%	2.9±1.4%
Motif 3	87.2±3.7%	40.9±6.2%	98.3±0.9%	97.1±1.5%

Comparison of the ratio of motifs after annealing to 400 K at lower coverage (0.013 ML) vs. high coverage (0.022 ML) demonstrates that the dehydrogenation reaction is coverage dependent, with a lower yield at higher initial coverage. A possible explanation for the observed trend is the stabilization within the supramolecular arrangements via van der Waals interactions between neighboring *tert*-butyl groups. At higher coverages around a full monolayer, practically all molecules are stabilized within an ordered island. On the other hand, at lower coverages 2D gas and ordered islands coexist. Thus, for the saturated monolayer dehydrogenation is less likely than in presence of a 2D gas phase. A similar coverage dependent dehydrogenation behavior has been observed for CuTPP on Cu(111) and has been attributed to intermolecular stabilizing effects as well.^[78]

In summary, the presented results highlight that porphyrins adsorbed on metal substrates are able to exhibit different *in situ* reactions, namely self-metalation and dehydrogenation, which have a significant influence on the adsorption behavior. So far, literature studies rather focused on the discussion if the self-metalation reaction of a free-base porphyrin takes place. From the presented experiments in the thesis at hand further insight into the self-metalation reaction could be determined. Interestingly, a modification of the self-metalation rate by peripheral CN-functionalization of tetraphenylporphyrin is found [P7]. Furthermore, a shift of the self-metalation temperature from 400 K to RT is induced by utilizing an open surface like Cu(110) compared to the more common Cu(111) substrate [P3]. Besides the self-metalation reaction, an *in situ* reaction of already metalated molecules is possible via an intramolecular dehydrogenation reaction [P2]. This kind of reaction offers the potential to influence macrocycle and periphery and thereby the adsorption behavior as a whole.

5. Conclusions

In the thesis at hand, the adsorption behavior of various tetraphenylporphyrins on different metal substrates, mainly based on STM investigations at or close to RT, has been discussed. The self-assembly of prototype functional molecules like porphyrins presents a versatile approach towards the fabrication of nanosystems and technological applications. The research in this field has led to the observation of diverse adsorption behaviors which presents a challenge to predict and to control the properties of such systems. However, it could be successfully demonstrated that, by close investigation and detailed discussion of the intramolecular conformation and supramolecular order of porphyrins adsorbed on metal substrates, certain fundamental patterns of molecule-molecule and molecule-substrate interactions can be distinguished and possibly exploited for the controlled fabrication of functional molecular architectures.

It could be demonstrated that tetraphenylporphyrins which exhibit a strong site specific molecule-substrate interaction adsorb as individual, isolated molecules on the surface while usually no long-range order is found. Such a strong interaction to substrate atoms can be established via the iminic nitrogens of free-base porphyrins like 2HTPP on Cu(111) leading to the observation of a novel, extremely distorted “inverted structure”. Isolated molecules and thus strong correlation with the substrate is also observed for CuTTBPP on Cu(110). The adsorption geometry of this molecule differs from the inverted structure and is rather flat-lying on the strongly corrugated Cu(110) substrate. In both cases, the absence of long-range ordered structures can be understood by a kinetic reason which is the limited diffusion of molecules at RT and partially also by the distorted conformation, which, e.g., do not allow for the common attractive T-type interactions in between tetraphenylporphyrins.

Supramolecular ordered structures can be induced by different measures, in particular by lifting the strong molecule-substrate interactions by metalation or by specific functionalization of the porphyrin periphery. In the latter regard in the framework of the thesis at hand cyano groups were tested for the first time. Functionalization of free-base tetraphenylporphyrin with cyano groups at the *para*-position of the phenyl legs leads to linear, one dimensional multimer structures on Cu(111). These structures form after a thermal treatment above RT and are facilitated by CN-Cu-CN metal-organic linking. In order to achieve supramolecular structures with two-dimensional order the strong interaction of free-base porphyrins with the substrate has to be reduced. This can be accomplished by either

modifying the substrate itself or introduction of steric hindrance within the molecule structure. For example the Cu(110) surface can be modified *in situ* by dosing oxygen. On the corresponding Cu(110)-(2x1)O substrate the molecule-substrate interaction is significantly reduced and the CuTTBPP molecules adsorb in two dimensional domains as compared to individual molecules on the bare substrate. For Cu(111) the strong interaction of free-base porphyrins and substrate was realized through the formation of the inverted structure. Tetrabenzoporphyrins present a class of molecules for which the inverted structure is inhibited by adding sterically demanding benzene rings to the pyrrole groups of the macrocycle. Thereby the interaction with the Cu(111) substrate is limited and the saddle shape adsorption geometry as well as two-dimensional supramolecular domains are observed. Generally, the supramolecular island structures are stabilized by molecule-molecule interactions like van der Waals, T-type and π - π stacking interactions. The specific properties of these 2D structures are determined by a complex interplay of molecule-molecule and molecule-substrate interactions. Therefore, the supramolecular domains can be further modified by functionalization of the periphery and/or the macrocycle center of the porphyrins.

A promising pathway to influence intramolecular conformation and supramolecular order of porphyrins *in situ* are reactions. Investigation of the self-metalation of free-base porphyrins on Cu(111) demonstrates that this reaction significantly changes the adsorption behavior by introducing a central metal atom. However, until recently few was known about the specifics of the self-metalation reaction and how to tailor these. From the results presented in the thesis at hand, a reduction of the self-metalation rate with increasing cyano group functionalization could be concluded. Furthermore a reduction of the reaction temperature from 400 K to RT is observed for 2HTTBPP on the more “open” Cu(110) surface compared to Cu(111). While the self-metalation functionalizes the central pocket of the molecule, the periphery can be modified by intramolecular dehydrogenation as observed for NiTTBPBP on Cu(111).

In conclusion, in the framework of the thesis at hand valuable, detailed insights into the adsorption behavior of porphyrins on metal substrates and in particular into the specific roles of molecule-molecule and molecule-substrate interactions are given. In this regard, the presented and discussed results indicate different strategies to influence the corresponding adsorption behaviors and thus suggest possibilities to tailor-make molecular architectures.

6. Zusammenfassung

Im Rahmen der vorliegenden Arbeit wurde das Adsorptionsverhalten unterschiedlicher Tetraphenylporphyrine (TPP) auf verschiedenen Metallsubstraten vorwiegend mittels Rastertunnelmikroskopie (engl. scanning tunneling microscopy, STM) bei oder nahe Raumtemperatur (RT) untersucht. Die Selbstassemblierung von komplexen Molekülen wie Porphyrinen stellt einen vielversprechenden Schritt zur Herstellung von Nanosystemen und deren technischer Anwendung dar. Da bei Untersuchungen auf diesem Gebiet verschiedene Adsorptionsverhalten beobachtet werden, ist es schwierig die Eigenschaften dieser Systeme vorherzusagen und zu kontrollieren. Durch genaue Untersuchungen und detaillierte Diskussion der intramolekularen Konformation sowie der supramolekularen Ordnung der auf Metalloberflächen adsorbierten Porphyrine können bestimmte grundlegende Zusammenhänge der Molekül-Molekül und Molekül-Substrat Wechselwirkungen unterschieden, und damit potentiell für die kontrollierte Herstellung funktioneller molekularer Architekturen benutzt werden.

Im Rahmen dieser Arbeit konnte gezeigt werden, dass Tetraphenylporphyrine, die eine ausgeprägte Molekül-Substrat Wechselwirkung aufweisen, als individuelle, isolierte Moleküle ohne weitreichende Ordnung auf der Oberfläche adsorbieren. Eine solche starke Wechselwirkung zu Substratatomten kann durch die iminischen Stickstoffatome von unmetallierten Porphyrinen wie 2HTPP auf Cu(111) realisiert werden. Weiterhin führte die starke Wechselwirkung zwischen Substrat und Molekül zur Beobachtung einer neuartigen intramolekularen Konformation, der extrem deformierten „invertierten Struktur“. Isolierte Moleküle, und die damit zusammenhängende starke Wechselwirkung mit dem Substrat, können auch für CuTTBPP auf Cu(110) beobachtet werden. Die Adsorptionsgeometrie dieses Moleküls unterscheidet sich von der invertierten Struktur und liegt eher flach auf dem stark korrigierten Cu(110) Substrat. In beiden Fällen kann das Fehlen von weitreichender Ordnung kinetisch begründet werden, da die Moleküle bei RT nur eingeschränkt diffundieren. Ein weiterer Grund ist die intramolekulare Konformation, die beispielsweise das Ausbilden von attraktiven „T-type“ Wechselwirkungen zwischen Tetraphenylporphyrinen verhindert.

Das Ausbilden von supramolekular geordneten Strukturen kann durch verschiedene Maßnahmen hervorgerufen werden. Im Vordergrund steht dabei das Aufheben der starken Molekül-Substrat Wechselwirkung durch Metallierung oder durch spezifische Funktionalisierung der Porphyrin-Peripherie. Zu Letzterem wurden im Rahmen der

vorliegenden Arbeit erstmalig Cyano-Gruppen getestet. Die Funktionalisierung von freie Base Tetraphenylporphyrinen mit Cyano-Gruppen an den *para*-Positionen der Phenylgruppen führt zu linearen, eindimensionalen Multimer-Strukturen auf Cu(111). Diese Strukturen bilden sich nach Heizen über RT und werden durch CN-Cu-CN Metall-organische Verknüpfungen gebildet. Für das Ausbilden von supramolekularen Strukturen mit zweidimensionaler Ordnung muss die starke Wechselwirkung zwischen freie Base Porphyrinen und dem Substrat verringert werden. Dies kann durch Modifikation des Substrats selbst oder dem Einbringen von sterischen Limitationen in der Molekülstruktur erreicht werden. Zum Beispiel kann die Cu(110) Oberfläche durch Dosieren von Sauerstoff *in situ* modifiziert werden. Auf der so entstandenen Cu(110)-(2x1)O Oberfläche ist die Molekül-Substrat Wechselwirkung deutlich verringert. Folglich adsorbieren CuTTBPP Moleküle in zweidimensionalen Domänen anstatt von individuellen Molekülen, wie auf dem nicht modifizierten Substrat beobachtet. Wie zuvor erläutert, kann auf Cu(111) die starke Wechselwirkung der, als freie Base vorliegenden, Porphyrine und dem Substrat durch die invertierte Struktur ausgebildet werden. Diesbezüglich stellen Tetrabenzoporphyrine eine Molekülklasse dar, für die, die Ausbildung der invertierten Struktur durch zusätzliche sterisch beanspruchende Benzolringe an den Pyrrolgruppen des Makrozyklus gehindert wird. Dadurch wird die Wechselwirkung mit dem Cu(111) Substrat limitiert und folglich werden für Tetrabenzoporphyrine eine „saddle shape“ Adsorptionsgeometrie wie auch zweidimensionale supramolekulare Domänen beobachtet. Grundsätzlich werden supramolekulare Inselstrukturen durch intermolekulare van der Waals, „T-type“ oder π - π Wechselwirkungen stabilisiert. Die genauen Eigenschaften dieser 2D Strukturen werden durch ein komplexes Zusammenspiel aus Molekül-Molekül und Molekül-Substrat Wechselwirkungen bestimmt. Daher können supramolekulare Domänen durch Funktionalisierung der Peripherie und/oder des Makrozyklus der Porphyrine weiterführend modifiziert werden.

Ein vielversprechender Weg zur Veränderung des Adsorptionsverhaltens von Porphyrinen liegt in *in situ* Reaktionen. Die Untersuchung der Selbstmetallierung (Metallierung mit Substratatomen) von Porphyrinen, die als freie Base vorliegen, auf Cu(111) zeigt, dass diese Reaktion das Adsorptionsverhalten durch Einsatz eines zentralen Metallatoms deutlich verändert. Allerdings ist bisher nur wenig über die Details der Selbstmetallierung, und wie man diese gezielt beeinflussen kann, bekannt. Aufgrund der in der vorliegenden Arbeit gezeigten Ergebnisse kann auf eine Reduzierung der Selbstmetallierungsrate mit

zunehmender Funktionalisierung durch Cyano-Gruppen zurück geschlossen werden. Außerdem wird eine Verringerung der Reaktionstemperatur für 2HTTBPP von 400 K auf Cu(111) zu RT auf der eher „offenen“ Cu(110) Oberfläche beobachtet. Während durch die Selbstmetallierung das Molekül zentral funktionalisiert werden kann, kann die Peripherie durch intramolekulare Dehydrogenierung, wie für NiTTBPBP auf Cu(111) beobachtet, funktionalisiert werden.

Somit konnten im Rahmen der vorliegenden Arbeit wertvolle, detaillierte Einblicke in das Adsorptionsverhalten von Porphyrinen auf Metallsubstraten, und insbesondere in die spezifischen Rollen der Molekül-Molekül als auch Molekül-Substrat Wechselwirkungen, gegeben werden. Die diskutierten Ergebnisse zeigen diesbezüglich verschiedene Herangehensweisen zur Beeinflussung des Adsorptionsverhaltens auf, und deuten somit verschiedene Möglichkeiten zur kontrollierten Herstellung molekularer Architekturen an.

7. Acknowledgement

The thesis at hand would have certainly been not possible without the support and help of a lot of people. I want to express my gratitude to:

PD Dr. Hubertus Marbach for excellent supervision and support on both scientific and personal level during my PhD time.

Professor Hans-Peter Steinrück for giving me the opportunity to do my PhD at his chair and providing outstanding scientific as well as social environment.

Professor Abner de Siervo who supervised me during my stay in Campinas. I want to thank him as well as Lucas Barreto, Rodrigo C.C. Ferreira and Luis Henrique de Lima for introducing me to and taking care of me in Brazil.

My colleagues from the STM lab, Liang Zhang, Michael Stark, Stefanie Ditze, Florian Buchner, Julia Köbl, Manuel Meusel and Gretel Siglreithmaier. I also want to thank the people who shared the office with me, Florian Vollnhals, Matthias Franke, Daniel Wechsler and Stephen Massicot.

My collaboration partners from theory, PD Dr. Wolfgang Hieringer, Professor Bernd Meyer and Martin Gurrath as well as from the physics department, Professor Alexander Schneider and Dr. Tobias Schmitt. The group of Professor Norbert Jux, especially Dr. Dominik Lungerich and Helen Hölzel, for synthesis of several porphyrins and being always open for discussions.

Hans-Peter Bäuml, Bernd Kress, Friedhold Wölfel and all the members of the mechanical workshop for their dedicated technical support as well as building or repairing various devices enabling outstanding experimental working conditions.

Besides my colleagues, I want to thank my parents and brothers and especially my partner Mel for their continuous, patient and unlimited support.

8. References

- [1] L. R. Milgrom, *The colours of life: an introduction to the chemistry of porphyrins and related compounds*. Oxford University Press **1997**.
- [2] H. Marbach, Habilitation treatise, *FAU Erlangen-Nürnberg* **2010**.
- [3] C. M. Carvalho, T. J. Brocksom, K. T. de Oliveira, Tetrabenzoporphyrins: synthetic developments and applications. *Chem. Soc. Rev.* **2013**, *42*, 3302-3317.
- [4] M. Grätzel, Dye-sensitized solar cells. *J. Photochem. Photobiol. C* **2003**, *4*, 145-153.
- [5] N. A. Rakow, K. S. Suslick, A colorimetric sensor array for odour visualization. *Nature* **2000**, *406*, 710-713.
- [6] J. P. Collman, P. Denisevich, Y. Konai, M. Marrocco, C. Koval, F. C. Anson, Electrode catalysis of the four-electron reduction of oxygen to water by dicobalt face-to-face porphyrins. *J. Am. Chem. Soc.* **1980**, *102*, 6027-6036.
- [7] C. Baddeley, Fundamental investigations of enantioselective heterogeneous catalysis. *Top. Catal.* **2003**, *25*, 17-28.
- [8] W. Auwärter, D. Ćija, F. Klappenberger, J. V. Barth, Porphyrins at interfaces. *Nat. Chem.* **2015**, *7*, 105-120.
- [9] J. V. Barth, Molecular architectonic on metal surfaces. *Annu. Rev. Phys. Chem.* **2007**, *58*, 375-407.
- [10] J. M. Gottfried, Surface chemistry of porphyrins and phthalocyanines. *Surf. Sci. Rep.* **2015**, *70*, 259-379.
- [11] H. Marbach, Surface-mediated in situ metalation of porphyrins at the solid-vacuum interface. *Acc. Chem. Res.* **2015**, *48*, 2649-2658.
- [12] R. Young, J. Ward, F. Scire, The topografiner: an instrument for measuring surface microtopography. *Rev. Sci. Instrum.* **1972**, *43*, 999-1011.
- [13] G. Binnig, H. Rohrer, C. Gerber, E. Weibel, Surface studies by scanning tunneling microscopy. *Phys. Rev. Lett.* **1982**, *49*, 57-61.
- [14] G. Binnig, H. Rohrer, C. Gerber, E. Weibel, 7×7 Reconstruction on Si(111) resolved in real space. *Phys. Rev. Lett.* **1983**, *50*, 120-123.
- [15] N. Yao, Z. L. Wang, *Handbook of microscopy for nanotechnology*, Springer **2005**.
- [16] R. Wiesendanger, T. Mulvey, Scanning probe microscopy and spectroscopy. *Meas. Sci. Technol.* **1995**, *6*, 600.
- [17] K. Oura, V. Lifshits, A. Saranin, A. Zotov, M. Katayama, *Surface science: an introduction*. Springer **2013**.
- [18] P. K. Hansma, J. Tersoff, Scanning tunneling microscopy. *J. Appl. Phys.* **1987**, *61*, R1-R24.
- [19] F. Buchner, K.-G. Warnick, T. Wölfle, A. Göring, H.-P. Steinrück, W. Hieringer, H. Marbach, Chemical fingerprints of large organic molecules in scanning tunneling microscopy: Imaging adsorbate–substrate coupling of metalloporphyrins. *J. Phys. Chem. C* **2009**, *113*, 16450-16457.
- [20] K. Comanici, F. Buchner, K. Flechtner, T. Lukasczyk, J. M. Gottfried, H.-P. Steinrück, H. Marbach, Understanding the contrast mechanism in scanning tunneling microscopy (STM) images of an intermixed tetraphenylporphyrin layer on Ag (111). *Langmuir* **2008**, *24*, 1897-1901.

8. References

- [21] I. Horcas et al., WSXM: a software for scanning probe microscopy and a tool for nanotechnology. *Rev. Sci. Instrum.* **2007**, *78*, 013705
- [22] R. González-Moreno, A. Garcia-Lekue, A. Arnau, M. Trelka, J. M. Gallego, R. Otero, A. Verdini, C. Sánchez-Sánchez, P. L. de Andrés, J. Á. Martín-Gago, C. Rogero, Role of the anchored groups in the bonding and self-organization of macrocycles: carboxylic versus pyrrole groups. *J. Phys. Chem. C* **2013**, *117*, 7661-7668.
- [23] R. González-Moreno, C. Sánchez-Sánchez, M. Trelka, R. Otero, A. Cossaro, A. Verdini, L. Floreano, M. Ruiz-Bermejo, A. García-Lekue, J. Á. Martín-Gago, C. Rogero, Following the metalation process of protoporphyrin IX with metal substrate atoms at room temperature. *J. Phys. Chem. C* **2011**, *115*, 6849-6854.
- [24] Z. X. Wang, F. H. Tian, The adsorption of O atom on Cu (100), (110), and (111) low-index and step defect surfaces. *J. Phys. Chem. B* **2003**, *107*, 6153-6161.
- [25] S. Ditze, Ph. D. thesis, *FAU Erlangen-Nürnberg* **2014**.
- [26] J. Steed, J. Atwood, *Supramolecular Chemistry*. Wiley & Sons **2009**.
- [27] G. Moss, Nomenclature of tetrapyrroles. *Pure Appl. Chem.* **1987**, *59*, 779-832.
- [28] F. Buchner, K. Comanici, N. Jux, H.-P. Steinrück, H. Marbach, Polymorphism of porphyrin molecules on Ag (111) and how to weave a rigid monolayer. *J. Phys. Chem. C* **2007**, *111*, 13531-13538.
- [29] F. Moresco, G. Meyer, K.-H. Rieder, J. Ping, H. Tang, C. Joachim, TBPP molecules on copper surfaces: a low temperature scanning tunneling microscope investigation. *Surf. Sci.* **2002**, *499*, 94-102.
- [30] F. Moresco, G. Meyer, K.-H. Rieder, H. Tang, A. Gourdon, C. Joachim, Conformational changes of single molecules induced by scanning tunneling microscopy manipulation: A route to molecular switching. *Phys. Rev. Lett.* **2001**, *86*, 672.
- [31] S. Ditze, M. Stark, F. Buchner, A. Aichert, N. Jux, N. Luckas, A. Görling, W. Hieringer, J. Hornegger, H.-P. Steinrück, H. Marbach, On the energetics of conformational switching of molecules at and close to room temperature. *J. Am. Chem. Soc.* **2014**, *136*, 1609-1616.
- [32] T. A. Jung, R. R. Schlittler, J. K. Gimzewski, Conformational identification of individual adsorbed molecules with the STM. *Nature* **1997**, *386*, 696-698.
- [33] W. Auwärter, F. Klappenberger, A. Weber-Bargioni, A. Schiffrin, T. Strunskus, C. Wöll, Y. Pennec, A. Riemann, J. V. Barth, Conformational adaptation and selective adatom capturing of tetrapyrrolyl-porphyrin molecules on a copper (111) surface. *J. Am. Chem. Soc.* **2007**, *129*, 11279-11285.
- [34] J. Brede, M. Linares, S. Kuck, J. Schwöbel, A. Scarfato, S. H. Chang, G. Hoffmann, R. Wiesendanger, R. Lensen, P. H. Kouwer, J. Hoogboom, A. E. Rowan, M. Broring, M. Funk, S. Stafstrom, F. Zerbetto, R. Lazzaroni, Dynamics of molecular self-ordering in tetraphenyl porphyrin monolayers on metallic substrates. *Nanotechnology* **2009**, *20*, 275602.
- [35] F. Buchner, I. Kellner, W. Hieringer, A. Görling, H.-P. Steinrück, H. Marbach, Ordering aspects and intramolecular conformation of tetraphenylporphyrins on Ag(111). *Phys. Chem. Chem. Phys.* **2010**, *12*, 13082-13090.
- [36] S. P. Jarvis, S. Taylor, J. D. Baran, D. Thompson, A. Saywell, B. Mangham, N. R. Champness, J. Larsson, P. Moriarty, Physisorption controls the conformation and density of states of an adsorbed porphyrin. *J. Phys. Chem. C* **2015**, *119*, 27982-27994.
- [37] K. Diller, F. Klappenberger, M. Marschall, K. Hermann, A. Nefedov, C. Wöll, J. V. Barth, Self-metalation of 2H-tetraphenylporphyrin on Cu(111): an x-ray spectroscopy study. *J. Chem. Phys.* **2012**, *136*, 014705.

- [38] F. Buchner, J. Xiao, E. Zillner, M. Chen, M. Röckert, S. Ditze, M. Stark, H.-P. Steinrück, J. M. Gottfried, H. Marbach, Diffusion, rotation, and surface chemical bond of individual 2H-tetraphenylporphyrin molecules on Cu(111). *J. Phys. Chem. C* **2011**, *115*, 24172-24177.
- [39] J. Xiao, S. Ditze, M. Chen, F. Buchner, M. Stark, M. Drost, H.-P. Steinrück, J. M. Gottfried, H. Marbach, Temperature-dependent chemical and structural transformations from 2H-tetraphenylporphyrin to Copper(II)-tetraphenylporphyrin on Cu(111). *J. Phys. Chem. C* **2012**, *116*, 12275-12282.
- [40] K. Flechtner, Ph. D. thesis, *FAU Erlangen-Nürnberg* **2007**.
- [41] F. Buchner, STM Investigation of molecular architectures of porphyrinoids on a Ag (111) surface: supramolecular ordering, electronic properties and reactivity. *Springer* **2010**.
- [42] R. Lindner, Ph. D. thesis, *FAU Erlangen-Nürnberg* **2004**.
- [43] K. Besocke, An easily operable scanning tunneling microscope. *Surf. Sci.* **1987**, *181*, 145-153.
- [44] G. E. Moore, Cramming more components onto integrated circuits. *Electronics* **1965**, *38*, 114-117.
- [45] G. Whitesides, J. Mathias, C. Seto, Molecular self-assembly and nanochemistry- A chemical strategy for the synthesis of nanostructures. *Science* **1991**, *254*, 1312-1319.
- [46] M. Gottfried, H. Marbach, Surface-confined coordination chemistry with porphyrins and phthalocyanines: Aspects of formation, electronic structure, and reactivity. *Z. Phys. Chem.* **2009**, *223*, 53-74.
- [47] J. V. Barth, Fresh perspectives for surface coordination chemistry. *Surf. Sci.* **2009**, *603*, 1533-1541.
- [48] F. Albrecht, F. Bischoff, W. Auwärter, J. V. Barth, J. Repp, Direct identification and determination of conformational response in adsorbed individual nonplanar molecular species using noncontact atomic force microscopy. *Nano Lett.* **2016**, *16*, 7703-7709.
- [49] W. Auwärter, A. Weber-Bargioni, A. Riemann, A. Schiffrin, O. Gröning, R. Fasel, J. V. Barth, Self-assembly and conformation of tetrapyridyl-porphyrin molecules on Ag(111). *J. Chem. Phys.* **2006**, *124*, 194708.
- [50] G. Rojas, X. Chen, C. Bravo, J.-H. Kim, J.-S. Kim, J. Xiao, P. A. Dowben, Y. Gao, X. C. Zeng, W. Choe, Self-assembly and properties of nonmetalated tetraphenyl-porphyrin on metal substrates. *J. Phys. Chem. C* **2010**, *114*, 9408-9415.
- [51] M. O. Sinnokrot, C. D. Sherrill, High-accuracy quantum mechanical studies of π - π interactions in benzene dimers. *J. Phys. Chem. A* **2006**, *110*, 10656-10668.
- [52] F. Buchner, E. Zillner, M. Röckert, S. Gläsel, H.-P. Steinrück, H. Marbach, Substrate-mediated phase separation of two porphyrin derivatives on Cu(111). *Chem. Eur. J.* **2011**, *17*, 10226-10229.
- [53] L. Grill, M. Dyer, L. Lafferentz, M. Persson, M. V. Peters, S. Hecht, Nano-architectures by covalent assembly of molecular building blocks. *Nat. Nanotechnol.* **2007**, *2*, 687-691.
- [54] S. Haq, F. Hanke, M. S. Dyer, M. Persson, P. Iavicoli, D. B. Amabilino, R. Raval, Clean coupling of unfunctionalized porphyrins at surfaces to give highly oriented organometallic oligomers. *J. Am. Chem. Soc.* **2011**, *133*, 12031-12039.
- [55] S. Haq, F. Hanke, J. Sharp, M. Persson, D. B. Amabilino, R. Raval, Versatile bottom-up construction of diverse macromolecules on a surface observed by scanning tunneling microscopy. *ACS Nano* **2014**, *8*, 8856-8870.

8. References

- [56] L. A. Fendt, M. Stöhr, N. Wintjes, M. Enache, T. A. Jung, F. Diederich, Modification of supramolecular binding motifs induced by substrate registry: formation of self-assembled macrocycles and chain-like patterns. *Chem. Eur. J.* **2009**, *15*, 11139-11150.
- [57] S. Gottardi, K. Müller, J. C. Moreno-López, H. Yildirim, U. Meinhardt, M. Kivala, A. Kara, M. Stöhr, Cyano-functionalized triarylamine on Au(111): competing intermolecular versus molecule/substrate interactions. *Adv. Mater. Interfaces* **2014**, *1*, 1300025.
- [58] D. Heim, D. Ecija, K. Seufert, W. Auwärter, C. Aurisicchio, C. Fabbro, D. Bonifazi, J. V. Barth, Self-assembly of flexible one-dimensional coordination polymers on metal surfaces. *J. Am. Chem. Soc.* **2010**, *132*, 6783-6790.
- [59] T. Yokoyama, S. Yokoyama, T. Kamikado, Y. Okuno, S. Mashiko, Selective assembly on a surface of supramolecular aggregates with controlled size and shape. *Nature* **2001**, *413*, 619-621.
- [60] K. Diller, A. C. Papageorgiou, F. Klappenberger, F. Allegretti, J. V. Barth, W. Auwärter, In vacuo interfacial tetrapyrrole metallation. *Chem. Soc. Rev.* **2016**, *45*, 1629-1656.
- [61] W. Hieringer, K. Flechtner, A. Kretschmann, K. Seufert, W. Auwärter, J. V. Barth, A. Görling, H.-P. Steinrück, J. M. Gottfried, The surface trans effect: influence of axial ligands on the surface chemical bonds of adsorbed metalloporphyrins. *J. Am. Chem. Soc.* **2011**, *133*, 6206-6222.
- [62] I. Mochida, K. Suetsugu, H. Fujitsu, K. Takeshita, K. Tsuji, Y. Sagara, A. Ohyoshi, A kinetic study on reduction of nitric oxide over cobalt tetraphenylporphyrin supported on titanium dioxide. *J. Catal.* **1982**, *77*, 519-526.
- [63] J. M. Gottfried, K. Flechtner, A. Kretschmann, T. Lukasczyk, H.-P. Steinrück, Direct synthesis of a metalloporphyrin complex on a surface. *J. Am. Chem. Soc.* **2006**, *128*, 5644-5645.
- [64] G. Di Santo, C. Sfiligoj, C. Castellarin-Cudia, A. Verdini, A. Cossaro, A. Morgante, L. Floreano, A. Goldoni, Changes of the molecule–substrate interaction upon metal inclusion into a porphyrin. *Chem. Eur. J.* **2012**, *18*, 12619-12623.
- [65] F. Buchner, K. Flechtner, Y. Bai, E. Zillner, I. Kellner, H.-P. Steinrück, H. Marbach, J. M. Gottfried, Coordination of iron atoms by tetraphenylporphyrin monolayers and multilayers on Ag (111) and formation of iron-tetraphenylporphyrin. *J. Phys. Chem. C* **2008**, *112*, 15458-15465.
- [66] W. Auwärter, A. Weber-Bargioni, S. Brink, A. Riemann, A. Schiffrin, M. Ruben, J. V. Barth, Controlled metalation of self-assembled porphyrin nanoarrays in two dimensions. *ChemPhysChem* **2007**, *8*, 250-254.
- [67] G. Di Santo, C. Castellarin-Cudia, M. Fanetti, B. Taleatu, P. Borghetti, L. Sangaletti, L. Floreano, E. Magnano, F. Bondino, A. Goldoni, Conformational Adaptation and Electronic Structure of 2H-Tetraphenylporphyrin on Ag(111) during Fe Metalation. *J. Phys. Chem. C* **2011**, *115*, 4155-4162.
- [68] A. Kretschmann, M.-M. Walz, K. Flechtner, H.-P. Steinrück, J. M. Gottfried, Tetraphenylporphyrin picks up zinc atoms from a silver surface. *Chem. Commun.* **2007**, *6*, 568-570.
- [69] T. E. Shubina, H. Marbach, K. Flechtner, A. Kretschmann, N. Jux, F. Buchner, H.-P. Steinrück, T. Clark, J. M. Gottfried, Principle and mechanism of direct porphyrin metalation: Joint experimental and theoretical investigation. *J. Am. Chem. Soc.* **2007**, *129*, 9476-9483.
- [70] A. Weber-Bargioni, J. Reichert, A. Seitsonen, W. Auwärter, A. Schiffrin, J. Barth, Interaction of cerium atoms with surface-anchored porphyrin molecules. *J. Phys. Chem. C* **2008**, *112*, 3453-3455.
- [71] D. Écija, W. Auwärter, S. Vijayaraghavan, K. Seufert, F. Bischoff, K. Tashiro, J. V. Barth, Assembly and manipulation of rotatable cerium porphyrinato sandwich complexes on a surface. *Angew. Chem. Int. Ed.* **2011**, *50*, 3872-3877.

- [72] M. Chen, X. Feng, L. Zhang, H. Ju, Q. Xu, J. Zhu, J. M. Gottfried, K. Ibrahim, H. Qian, J. Wang, Direct synthesis of nickel (II) tetraphenylporphyrin and its interaction with a Au (111) surface: a comprehensive study. *J. Phys. Chem. C* **2010**, *114*, 9908-9916.
- [73] C. M. Doyle, S. A. Krasnikov, N. N. Sergeeva, A. B. Preobrajenski, N. A. Vinogradov, Y. N. Sergeeva, M. O. Senge, A. A. Cafolla, Evidence for the formation of an intermediate complex in the direct metalation of tetra(4-bromophenyl)-porphyrin on the Cu(111) surface. *Chem. Commun.* **2011**, *47*, 12134-12136.
- [74] A. Goldoni, C. A. Pignedoli, G. Di Santo, C. Castellarin-Cudia, E. Magnano, F. Bondino, A. Verdini, D. Passerone, Room temperature metalation of 2H-TPP monolayer on iron and nickel surfaces by picking up substrate metal atoms. *ACS Nano* **2012**, *6*, 10800-10807.
- [75] S. Ditze, M. Stark, M. Drost, F. Buchner, H.-P. Steinrück, H. Marbach, Activation energy for the self-metalation reaction of 2H-tetraphenylporphyrin on Cu(111). *Angew. Chem. Int. Ed.* **2012**, *51*, 10898-10901.
- [76] H. Marbach, H.-P. Steinrück, Studying the dynamic behaviour of porphyrins as prototype functional molecules by scanning tunnelling microscopy close to room temperature. *Chem. Commun.* **2014**, *50*, 9034-9048.
- [77] M. Röckert, S. Ditze, M. Stark, J. Xiao, H.-P. Steinrück, H. Marbach, O. Lytken, Abrupt coverage-induced enhancement of the self-metalation of tetraphenylporphyrin with Cu(111). *J. Phys. Chem. C* **2014**, *118*, 1661-1667.
- [78] M. Röckert, M. Franke, Q. Tariq, S. Ditze, M. Stark, P. Uffinger, D. Wechsler, U. Singh, J. Xiao, H. Marbach, H.-P. Steinrück, O. Lytken, Coverage- and temperature-dependent metalation and dehydrogenation of tetraphenylporphyrin on Cu(111). *Chem. Eur. J.* **2014**, *20*, 8948-8953.
- [79] M. Röckert, M. Franke, Q. Tariq, D. Lungerich, N. Jux, M. Stark, A. Kaftan, S. Ditze, H. Marbach, M. Laurin, Insights in reaction mechanistic: Isotopic exchange during the metalation of deuterated Tetraphenyl-21, 23 D-porphyrin on Cu (111). *J. Phys. Chem. C* **2014**, *118*, 26729-26736.
- [80] Y. He, M. Garnica, F. Bischoff, J. Ducke, M. L. Bocquet, M. Batzill, W. Auwärter, J. V. Barth, Fusing tetrapyrroles to graphene edges by surface-assisted covalent coupling. *Nat. Chem.* **2017**, *9*, 33-38.
- [81] G. Rojas, S. Simpson, X. Chen, D. A. Kunkel, J. Nitz, J. Xiao, P. A. Dowben, E. Zurek, A. Enders, Surface state engineering of molecule–molecule interactions. *Phys. Chem. Chem. Phys.* **2012**, *14*, 4971-4976.
- [82] F. Klappenberger, A. Weber-Bargioni, W. Auwärter, M. Marschall, A. Schiffrin, J. V. Barth, Temperature dependence of conformation, chemical state, and metal-directed assembly of tetrapyrrolyl-porphyrin on Cu(111). *J. Chem. Phys.* **2008**, *129*, 214702.
- [83] C. Bürker, A. Franco-Cañellas, K. Broch, T.-L. Lee, A. Gerlach, F. Schreiber, Self-metalation of 2H-Tetraphenylporphyrin on Cu (111) studied with XSW: Influence of the central metal atom on the adsorption distance. *J. Phys. Chem. C* **2014**, *118*, 13659-13666.
- [84] M. Stark, S. Ditze, M. Lepper, L. Zhang, H. Schlott, F. Buchner, M. Rockert, M. Chen, O. Lytken, H.-P. Steinrück, H. Marbach, Massive conformational changes during thermally induced self-metalation of 2H-tetrakis-(3,5-di-tert-butyl)-phenylporphyrin on Cu(111). *Chem. Commun.* **2014**, *50*, 10225-10228.
- [85] S. Mohnani, D. Bonifazi, Supramolecular architectures of porphyrins on surfaces: The structural evolution from 1D to 2D to 3D to devices. *Coord. Chem. Rev.* **2010**, *254*, 2342-2362.
- [86] U. Schlickum, R. Decker, F. Klappenberger, G. Zoppellaro, S. Klyatskaya, W. Auwärter, S. Neppl, K. Kern, H. Brune, M. Ruben, Chiral kagomé lattice from simple ditopic molecular bricks. *J. Am. Chem. Soc.* **2008**, *130*, 11778-11782.

8. References

- [87] M. Stöhr, S. Boz, M. Schar, M. T. Nguyen, C. A. Pignedoli, D. Passerone, W. B. Schweizer, C. Thilgen, T. A. Jung, F. Diederich, Self-assembly and two-dimensional spontaneous resolution of cyano-functionalized [7]helicenes on Cu(111). *Angew. Chem. Int. Ed.* **2011**, *50*, 9982-9986.
- [88] J. I. Urgel, D. Ecija, W. Auwärter, D. Stassen, D. Bonifazi, J. V. Barth, Orthogonal insertion of lanthanide and transition-metal atoms in metal-organic networks on surfaces. *Angew. Chem. Int. Ed.* **2015**, *54*, 6163-6167.
- [89] C. Perry, S. Haq, B. Frederick, N. Richardson, Face specificity and the role of metal adatoms in molecular reorientation at surfaces. *Surf. Sci.* **1998**, *409*, 512-520.

9. Appendix

9.1 List of Figure Raw Data

Fig 2.1	100118_2	Fig 4.14 (right, top)	150424_61
Fig 4.3 (c)	161124_42-82	Fig 4.14 (right, bottom)	150429_54
Fig 4.4	150528_60-110	Fig 4.15 (a)	150415_19
Fig 4.5 (a)	140117_17	Fig 4.15 (b)	150415_105
Fig 4.5 (b)	140124_10-52	Fig 4.15 (d),(e)	150417_47
Fig 4.6 (a)	140624_12-65	Fig 4.16 (a)	131108_20
Fig 4.6 (b)	140627_99	Fig 4.16 (b)	131107_90-117
Fig 4.6 (c)	140627_182	Fig 4.16 (c)	131111_26
Fig 4.7 (left side)	141222_102	Fig 4.16 (d)	140124_10-52
Fig 4.7 (right side)	141126_74	Fig 4.17 (a)	140624_9
Fig 4.8 (a),(c)	150320_56	Fig 4.17 (b)	140624_12-65
Fig 4.9	141126_74	Fig 4.18 (a)	160308_32
Fig 4.10 (a)	150319_69	Fig 4.18 (b)	160309_8
Fig 4.10 (b),(c)	150320_56	Fig 4.18 (c)	160309_117
Fig 4.12 (a)	161115_18	Fig 4.18 (d)	160310_49
Fig 4.12 (b)	161115_58	Fig 4.20 (left side)	141222_102
Fig 4.12 (c)	150507_34-67	Fig 4.20 (middle)	141126_74
Fig 4.13 (a)	160128_9-41	Fig 4.20 (right side)	150323_44
Fig 4.13 (b)	160428_134-166	Fig 4.21 (a)	140627_197
Fig 4.13 (c)	150903_82	Fig 4.21 (b)	140627_195
Fig 4.13 (d)	150507_34-67	Fig 4.21 (c)	140704_60
Fig 4.14 (left, top)	150415_105	Fig 4.21 (d)	140704_20
Fig 4.14 (left, bottom)	150410_52		

9.2 Publications [P1-7]

[P1] Role of Specific Intermolecular Interactions for the Arrangement of Ni(II)-5, 10, 15, 20-Tetraphenyltetrabenzoporphyrin on Cu(111)

Michael Lepper, Liang Zhang, Michael Stark, Stefanie Ditze, Dominik Lungerich, Norbert Jux, Wolfgang Hieringer, Hans-Peter Steinrück and Hubertus Marbach

J. Phys. Chem. C. **2015**, 119, 19897-19905

[P2] Self-assembly and coverage dependent thermally induced conformational changes of Ni(II)-mesotetrakis(4-tert-butylphenyl) benzoporphyrin on Cu(111)

Liang Zhang, Michael Lepper, Michael Stark, Dominik Lungerich, Norbert Jux, Wolfgang Hieringer, Hans-Peter Steinrück and Hubertus Marbach

Phys. Chem. Chem. Phys. **2015**, 17, 13066-13073

[P3] 2H-Tetrakis(3,5-di-tert-butyl)phenylporphyrin on a Cu(110) Surface: Room-Temperature Self-Metalation and Surface-Reconstruction-Facilitated Self-Assembly

Liang Zhang, Michael Lepper, Michael Stark, Ralf Schuster, Dominik Lungerich, Norbert Jux, Hans-Peter Steinrück and Hubertus Marbach

Chem. Eur. J. **2016**, 22, 3347-3354

[P4] On the critical role of the substrate: the adsorption behaviour of tetrabenzoporphyrins on different metal surfaces

Liang Zhang, Michael Lepper, Michael Stark, Teresa Menzel, Dominik Lungerich, Norbert Jux, Wolfgang Hieringer, Hans-Peter Steinrück and Hubertus Marbach

Phys. Chem. Chem. Phys. **2017**, 19, 20281-20289

[P5] “Inverted” porphyrins: a distorted adsorption geometry of free-base porphyrins on Cu(111)

Michael Lepper, Julia Köbl, Tobias Schmitt, Martin Gurrath, Abner de Siervo, M. Alexander Schneider, Hans-Peter Steinrück, Bernd Meyer, Hubertus Marbach and Wolfgang Hieringer

Chem. Commun. **2017**, 53, 8207-8210

[P6] Adsorption Behavior of a Cyano-Functionalized Porphyrin on Cu(111) and Ag(111): From Molecular Wires to Ordered Supramolecular Two-Dimensional Aggregates

Michael Lepper, Tobias Schmitt, Martin Gurrath, Marco Raschmann, Liang Zhang, Michael Stark, Helen Hölzel, Norbert Jux, Bernd Meyer, M. Alexander Schneider, Hans-Peter Steinrück and Hubertus Marbach

J. Phys. Chem. C, **2017**, 121, 26361-26371

[P7] Controlling the Self-Metalation Rate of Tetraphenylporphyrins on Cu(111) via Cyano Functionalization

Michael Lepper, Julia Köbl, Liang Zhang, Manuel Meusel, Helen Hölzel, Norbert Jux, Bernd Meyer, Abner de Siervo, Hans-Peter Steinrück and Hubertus Marbach

Accepted by Angew. Chem. Int. Ed., DOI: 10.1002/anie.201803601